NASA TECHNICAL MEMORANDUM

UB
NASA TM X-1667

PRELIMINARY STUDY OF A SUBSONIC NUCLEAR CRUISE AIRPLANE HAVING A HELIUM-COOLED THERMAL REACTOR

by John L. Allen, Laurence H. Fishbach
and William C. Strack

Lewis Research Center
Cleveland, Ohio

NATIONAL AERONAUTICS AND SPACE ADMINISTRATION • WASHINGTON, D. C. • OCTOBER 1968

NASA TM X-1667

PRELIMINARY STUDY OF A SUBSONIC NUCLEAR CRUISE AIRPLANE

HAVING A HELIUM-COOLED THERMAL REACTOR, *preliminary study.(U)*

By John L. Allen, Laurence H. Fishbach, and William C. Strack

Lewis Research Center
Cleveland, Ohio

Classification canceled (or changed to *Unclassified.*)
by authority of *Th. N. Maines, NASA Hq. Ltr. 25 Jan. 72* by
Name and grade of officer authorizing change
Gloria Zamora GS2 Feb. 15, 1972
Name & Grade of Officer making change

GROUP 4
Downgraded at 3 year intervals,
declassified after 12 years

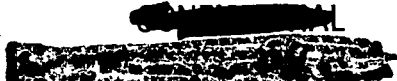## NATIONAL AERONAUTICS AND SPACE ADMINISTRATION

ABSTRACT

The combinations of nuclear, propulsion, and airframe components, related by 12 independent variables, that yielded maximum payload are presented for various flight cruise points. A unit shield which minimized maintenance and operational problems, was designed to limit the flight crew dose to 2.5 rem per 1000 hours of flight. Crash safety and afterheat removal problems were not assessed. Payload fraction increased at a declining rate as gross weight increased. The value was 5 percent for a 1/2-million-pound (22.7×10^4-kg) airplane and increased to 19 and 22 percent, respectively, for 1- and $1\frac{1}{4}$-million-pound (45.4×10^4- and 56.7×10^4-kg) airplanes designed for Mach 0.8 at 36 000 feet (10 970 m). Comparison with the C-5A class of airplanes at equal gross weights (7.3×10^5 lb; 3.3×10^5 kg) indicates superior payloads for the nuclear plane at all ranges beyond 5900 miles ($\sim11\times10^6$ m) for one-way trips, or 2700 miles ($\sim5\times10^6$ m) for round trips without refueling. The important characteristics of major components are described, as well as the trade-off networks occurring in determining the best payloads.

ii

CONTENTS

PRELIMINARY STUDY OF A SUBSONIC NUCLEAR CRUISE AIRPLANE
HAVING A HELIUM-COOLED THERMAL REACTOR*

by John L. Allen, Laurence H. Fishbach, and William C. Strack

Lewis Research Center

SUMMARY

A preliminary design-point study of a subsonic aircraft powered during cruise by a helium-cooled thermal nuclear reactor has been conducted. The crew radiation dose of 2.5 rem for 1000 hours of flight duty per year is only one-half the yearly dose recommended by the Federal Radiation Council. A unit shield was used to minimize maintenance and operational problems usually associated with this type of aircraft proposal.

Both metal-water and hydride-water shields were considered, as well as various packing factors representing the ratio of fabricated to ideal shield weight. Crash safety and afterheat removal weight penalties have not been assessed. The maximum helium temperature was limited to 2360° R (1311 K), and the nominal maximum reactor wall temperature was fixed at 2560° R (1422 K). Twelve independent variables were used to relate nuclear, propulsion, and airframe components so that a maximized figure of merit would include trade-off effects.

Results indicate attractive payloads for most speed and altitude design conditions, if the gross weight is large enough. Payload fraction increased with gross weight at a declining rate. The value for a 1/2-million-pound (22.7×10^4 kg) airplane was 5 percent and increased to 19 and 22 percent, respectively, for 1- and $1\frac{1}{4}$-million-pound (45.4×10^4- and 56.7×10^4-kg) airplanes designed for Mach 0.8 at 36 000 feet (10 970 m). Comparison with the C-5A class of airplanes at equal gross weights ($\sim 7.3 \times 10^5$ lb; 3.3×10^5 kg) indicates superior payloads for the nuclear plane for ranges beyond 5900 nautical miles ($\sim 11 \times 10^6$ m) for one-way trips or 2700 nautical miles ($\sim 5 \times 10^6$ m) for round trips without refueling. The payload for the nuclear aircraft could possibly be increased as much as 50 percent with shield technology advances which are unique to the nuclear concept. Other technology benefits could be mutually used by the two types of airplanes.

Payloads varied only 7 percent for turbine inlet temperatures between 1800° and 2100° R (1000 and 1166 K) and $1\frac{1}{2}$ percent for helium pressures between 1600 and 2000 psi (11×10^6 and 13.8×10^6 N/m^2) because other component designs were allowed to reoptimize for maximum payload. Because of the higher efficiency of the turbofan cycle, its payload was 108 to 16 percent greater than for the turbojet depending on the design flight Mach number.

*Title unclassified.

INTRODUCTION

Nuclear-powered aircraft today, as in the past, promise essentially unlimited endurance or range. The extensive work of the past ANP (aircraft nuclear propulsion) program (ref. 1) did not lead to the production of a usable airplane. Other studies such as CAMAL (continuously airborne missile launcher and low level weapon system), the logistic work of references 2 and 3, continued to examine the mission application. The projects underwent a transition from weapon system to component Advanced Development Objectives to eventual cancellation. Nevertheless, as suggested in reference 4, periodic reevaluation of performance potential is justified because of advancing technology, new ideas, and new mission needs.

Some of the changes in technology and application suggest that nuclear aircraft appear more feasible than indicated by earlier efforts (also see ref. 5):

(1) The ability to build very large aircraft, such as the C-5A, favors the nuclear system. Shield weight, which is the major weight fraction of the propulsive system, increases at less than a linear rate with power and therefore favors the larger gross weights.

(2) Present mission emphasis is for subsonic endurance in excess of 50 hours and for large cargo capacities or space for outsize items. Since supersonic capability is not required, the installed reactor power, and hence engine size and shield weight, is much less because of the better lift-drag ratio and lower velocity. Also, the temperature margin between the reactor fluid and the turbine air is greater since the ram temperature rise of supersonic flight is avoided.

(3) Similarly, the ability to build a variety of efficient fanjet engines (high bypass and compressor pressure ratios, if needed) helps reduce installed power and size.

(4) Knowledge concerning shield design techniques and materials has improved. Therefore, a general reduction of radiation hazard may be realized by specifying a unit shield and a low dose rate. The ground handling and maintenance would be greatly simplified. Furthermore, the smaller core associated with the choice of a closed-loop system using a high-capacity heat-transfer system such as helium or liquid metals (ref. 2) means that the unit shield can be lighter than for the open-direct-air method.

The objective herein is to illustrate or identify as a first step the relative importance and characteristics of major components and their interrelations and sensitivity factors. Some estimate of the expected payload weight fraction, delivery rate, and engine and aircraft design will also be given. However, because of the complexity of a nuclear propulsion system, definitive evaluation requires detailed knowledge about many components which is not presently available. The results, then, will form the basis for more refined calculations as better information on components becomes available. The scope of this design-point preliminary study has been limited to a unit-shielded helium-cooled thermal reactor using turbojet or turbofan propulsion in a subsonic logistic type

aircraft. The dose rate has been set at 2.5 millirem per hour at the flight deck, which for a 1000-hour tour of flight duty is well below the Federal Radiation Council limit of 5 rem per year per individual. Aircraft size was varied from 1/2 to $1\frac{1}{4}$ million pounds (22.7×10^4 to 56.7×10^4 kg). A computer program was utilized to trade off simultaneously the performance-weight advantages of as many as 12 major design parameters in order to maximize a selected figure of merit, such as payload.

The engines were assumed to have a tandem arrangement of the heat exchanger and chemical (fossil) fuel burner located between the compressor and turbine and within the turbine frontal area. The burner was used during the noncruise portions of the flight. Simultaneous chemical-nuclear operation was not evaluated. Safety or afterheat removal problems were not considered and any related weight penalties would have to be deducted from the payloads given herein.

SYMBOLS

A	area
AR	aspect ratio
A/A*	one-dimensional area ratio
A_i	ratio of wetted surface to wing area
A_0	total engine stream tube area
B	maximum fuselage width
BPR	fan jet bypass ratio = $\dfrac{\text{fan}}{\text{gas generator}}$ flow
b	wing span
b_s	structural wing span
C	constant
C_D	drag coefficient
$C_{D,i}$	coefficient of drag due to lift
$C_{D,o}$	coefficient of profile drag
$C_{D,total}$	coefficient of total drag
C_{fr}	coefficient of friction
C_i	thickness ratio correction factor

C_L	lift coefficient
C_p	specific heat at constant pressure
$C_{r,o}$	roughness coefficient, 0.0005
c_r	wing root chord
D_d	dose distance between reactor and flight deck
D_{fan}	diameter of total airflow stream tube
D_{tip}	diameter of gas generator airflow stream tube
d_f	maximum fuselage depth
ΔE	change in total aircraft energy during climb
e	aircraft specific energy
F	thrust
$F/\dot{w}_a$	thrust per pound of total airflow
F_{inst}	installed thrust
F_{SLS}	sea-level static thrust
f	correlation factor
H	altitude
HV	fuel heating value
IV	independent variable
KE	kinetic energy
$K_{C_{L,\alpha}}$	proportionality constant between lift and drag due to lift
K_f	wing quarter chord intersect location, percent of l_f
L	lift
L/D	cruise design lift to drag ratio
l_c	length of cargo compartment
l_f	fuselage length
l_i	characteristic length of a component
M_0	flight Mach number
N	number of engines
n_f	ultimate load factor, 1.5×2.5

P	pressure
ΔP	pressure drop
ΔP_{duct}	helium pressure drop in duct
ΔP_{HX}	helium pressure drop in heat exchanger
PE	potential energy
PR	pressure ratio across pump
P_{He}	helium pressure out of pump
P_{in}	reactor inlet helium pressure, psia; N/m^2
P_2/P_1	fan pressure ratio
P_3/P_1	overall pressure ratio
P_4/P_3	heat exchanger air-side pressure ratio
$\mathscr{P}$	reactor power, MW
$\mathscr{P}_p$	pump power, MW
Q_p	correction for variation of profile drag with lift
Q_Λ	sweepback correction to induced drag
Q_λ	correction for nonelliptical induced drag
q_0	dynamic pressure, lb/ft^2; N/m^2
R	range, miles; m (also gas constant for air)
RC	rate of climb, ft/min; m/min
R_s	outer radius of shield, $R_c = R_{sh}$ when shield is external to cargo bay
R_{sh}	when reactor is within cargo bay, $R_{sh} = 0$
S_f	fuselage wetted surface area
S_{ht}	planform area of horizontal area
S_N	nacelle and pylon wetted area
S_{vt}	planform area of vertical tail
S_w	wing planform area, ft^2; m^2
T	temperature, ^{O}R; K
ΔT	temperature rise across reactor
T_{ex}	reactor exit helium temperature

$T_{He, max}$	maximum helium temperature, 2360° R; 1311 K
T_{HX}	heat exchanger exit helium temperature
T_{in}	pump exit (reactor inlet) temperature
$T_{R, wall}$	nominal maximum reactor wall temperature, 2560° R; 1422 K
$T_{wall, max}$	maximum heat exchanger wall temperature
T_4	heat exchanger exit air temperature and turbine inlet temperature without chemical burning
t	time
t_r	maximum wing root thickness
V_{app}	landing approach velocity, ft/sec; m/sec
V_0	flight velocity, ft/sec; m/sec
W	weight (mass), lb; kg
W/A	helium flowrate per unit free flow in reactor
W_{crew}	weight of crew
W_{eng}	weight of engines
W_F	weight of chemical fuel
$W_{F, TC}$	weight of chemical fuel used from takeoff to cruise
$W_{F+tanks}$	weight of chemical fuel and tanks
$W_{f, a}$	available fuselage load
$W_{f, l}$	total load causing bending moment at wing root
W_{fix}	weight of fixed equipment and systems such as instruments, communications, controls, hydraulic, electric, APU's, etc.
W_{fuse}	weight of fuselage
W_g	gross weight
W'_g	weight at beginning of nuclear cruise
W_{gear}	landing gear weight
W_{HX}	weight of heat exchangers
W_{HXL}	weight of heat exchangers plus ducts
W_L	weight of payload
W_{lines}	weight of helium lines (ducts)

W_N	nacelle and pylon weight
W_{pp}	weight of powerplant
W_{prov}	weight of provisions
W_{pump}	weight of pump
W_s	weight of shield
W_{s+p}	weight of shield plus penetration penalty
$W_{s+p+rea}$	weight of shield plus penetration penalty plus reactor
W_{str}	weight of structure (includes equipment and systems)
W_{sum}	weight of $W_F + W_{eng} + W_{HX} + W_{lines}$
W_t	tail weight
W_{tanks}	additive wing weight to account for chemical fuel containment
W_w	wing weight
$W_{w,a}$	available wing load
$\dot{w}$	flow rate, lb/sec; kg/sec
$X_{1/4}$	longitudinal distance between the quarter chord intercept at the center line and at the mean aerodynamic chord
α	ratio of stream static pressure to sea level static pressure
β	exponent
γ	ratio of specific heats
δ_0	ratio of stream total to sea level static pressure, $P_0/2116$ lb/ft^2; $P_0/10.13 \times 10^4$ N/m^2
η_{oa}	overall engine efficiency
η_p	pump polytropic efficiency
θ_0	ratio of stream total to sea level static temperature, $T_0/518.6^o$ R; $T_0/288.3$ K
Λ	wing sweepback angle
$\Lambda_{1/4}$	wing sweepback angle, quarter chord
λ	wing planform taper ratio
ψ	ratio of stream static to sea level static temperature
σ	stress, psi; N/m^2 (also flight path angle)

τ	thickness to chord ratio
$\tau_{w, \perp, 1/4}$	wing thickness to chord ratio perpendicular to wing quarter chord line
φ	packing factor, shield weight multiple

Subscripts:

a	air
c	cruise
d	descent
des	design
He	helium
HX	heat exchanger
o	reference point values
rea	reactor
s	shield
T	total

Superscript:

—	average value between end of takeoff and cruise

METHOD OF ANALYSIS

General Requirements and Goal

This section presents some background concerning the problems and choices made for the nuclear system, propulsion system, and mission.

General arrangement of a nuclear propulsive system. - Figure 1 defines the particular closed-loop helium nuclear propulsion system considered. Fundamentally, heat is transferred to the working fluid from the surfaces of the reactor fuel elements; the fluid is pumped through pipes or ducts to a heat exchanger where air from the compressor of the propulsive device is heated prior to driving a turbine. A biological radiation shield, shown here as a unit type, protects selected regions. Some special arrangement for penetrating the shield with the working fluid ducts and preventing radiation from "seeing through" the duct is needed and is shown here as a half-turn helix.

Although the typical arrangement of a nuclear propulsive system described previously seems very simple, the design of the complete system is complicated by the interfaces between major components. In a general sense, a performance-weight map exists for a family of designs for each major component. However, before overall vehicle per-
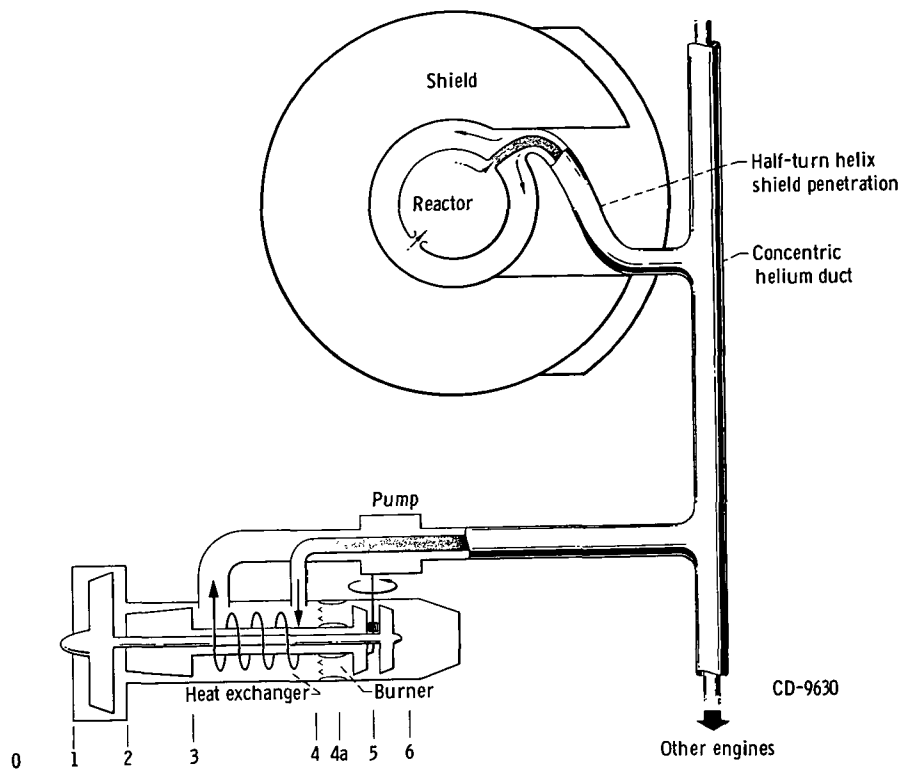
Figure 1. - Schematic of closed-loop nuclear propulsion system.

formance can be estimated, the component design points must be established after allowing interaction between components. Thus, the selected figure of merit for the complete system can be maximized rather than trying to assemble independently optimized components. The component performance-weight maps used in this study are based on unpublished preliminary Lewis data.

A logistics airplane was selected for this study. This choice of a logistic rather than an endurance type subsonic airplane for performance estimation was arbitrary. However, the logistic missions do not require consideration of such a broad range of design points, payloads, fuselage sizes, etc. as the endurance type. The logistics aircraft may well fulfill some endurance applications, but, in general, it is inherently compromised by the large and heavy cargo fuselage.

An ideal logistics airplane that has almost unlimited range should also be large enough to contain outsize items of military equipment as well as the ability to carry an appreciable load. As previously stated in the INTRODUCTION section, the variation of shield weight with nuclear power favors large airplanes. For these reasons, the base-point gross weight was selected as 1 million pounds (45.4×10^4 kg) or somewhat larger than the C-5A.

The choice of a closed-loop helium coolant system for transferring heat from the reactor to the air in the propulsive system is compatible with the goal of very low radiation levels, since helium does not become activated. Furthermore, helium is chemically inert, has excellent heat-transfer characteristics at high pressures, but has microscopic leakage problems, as well as the explosion hazard of pressurized gas systems.

After trial calculations, the heat exchanger was fitted within the turbine frontal area and between the compressor and turbine rather than duct air to heat exchangers in a more remote location. A burner for chemical fuel was included in tandem downstream of the exchanger. The resulting arrangement displays shaft and bearing problems only slightly greater than those encountered when scroll ducts are fitted to the engine to transfer air to and from a heat exchanger in a remote location.

Since the engine weight penalty is nearly the same, ducting a good heat-transfer fluid to the heat exchanger seems more logical because a greater variety of aircraft arrangements are possible due to the smaller duct sizes.

Since nuclear operation is contemplated only for the cruise portion, the chemical burner was incorporated for emergency operations and for the takeoff, climb to cruise, letdown, and landing segments of the flight. The noncruise parts of the flight path have been given only cursory study since this report is primarily a design-point study. However, the procedures adopted are believed to be better than assigning typical values for items such as fossil fuel weight.

Thus, a subsonic logistic turbofan or turbojet aircraft of 1 million pounds $(45.4 \times 10^4$ kg) gross weight powered by a unit-shielded helium-cooled thermal nuclear reactor with heat exchangers integral with the engine has been selected as a conceptual configuration. The goal is to use such a configuration as a model for reflecting relative importance, characteristics, interrelations, and sensitivity factors of major components, as well as defining areas of interest for airplane design-point performance and size.

System figure of merit and synthesis. - For the logistics mission, the figure of merit for the virtually unlimited range nuclear aircraft system is payload or, in some cases, delivery rate, which is the product of payload and velocity. The system weight synthesis is composed of three primary parts: the payload, aircraft structure, and the powerplant. The composition of these primary parts is as follows:

Powerplant:
    Engines, with helium pump
    Heat exchangers
    Helium ducting
    Reactor with pressure vessel
    Shield and penetration penalty
    Chemical fuel supply
    Allowance for moderator, shield, and after-heat cooling system

Structure:
    Wing
    Fuselage
    Nacelles and pylons
    Tail
    Landing gear
    Fixed equipment and systems
Payload:
    Cargo
    Crew
    Provisions

Powerplant

Turbomachinery. - Station designations are shown on the schematic in figure 1 which can represent either the turbofan or turbojet engine. For compressor pressure ratios less than 8, a single spool turbojet is considered for engine weight estimation. Otherwise, two-spool units are employed for either the turbofan (one fan spool, one compressor spool) or the turbojet. The relations used for estimating the engine weight and the values used for component efficiency are detailed in appendix A.

The tandem arrangement of the coolant-to-air heat exchanger and the chemical fuel burner permits operation at a higher turbine inlet temperature than would be possible using only nuclear power. Augmented turbine temperature operation is employed for takeoff and climb to cruise, and it is discussed subsequently in the Airplane Configuration and Operating Assumptions section. The power required to pump the helium is removed as shaft power from each engine.

Reactor. - The model selected for the nuclear power source was a helium-cooled thermal reactor with water moderation using refractory metal fuel elements at a nominal maximum metal wall temperature of 2560° R (1422 K). A sample performance map of the reactor family is illustrated in figure 2 for the standard conditions used throughout the report, unless specified, of a reactor inlet pressure of 1750 psia (12.06×10^6 N/m^2) and an outlet temperature of 2360° R (1311 K). Values of the helium weight flow per unit flow area at various power levels are plotted against reactor radius (which is outside the reflectors) and a correlation parameter f used in the shield weight calculation.

Reactor performance calculations usually require long periods of computer time and are not suited for the optimization procedure used herein which may require several hundred reactor iterations for a single design point. The curve fits and Taylor expan-
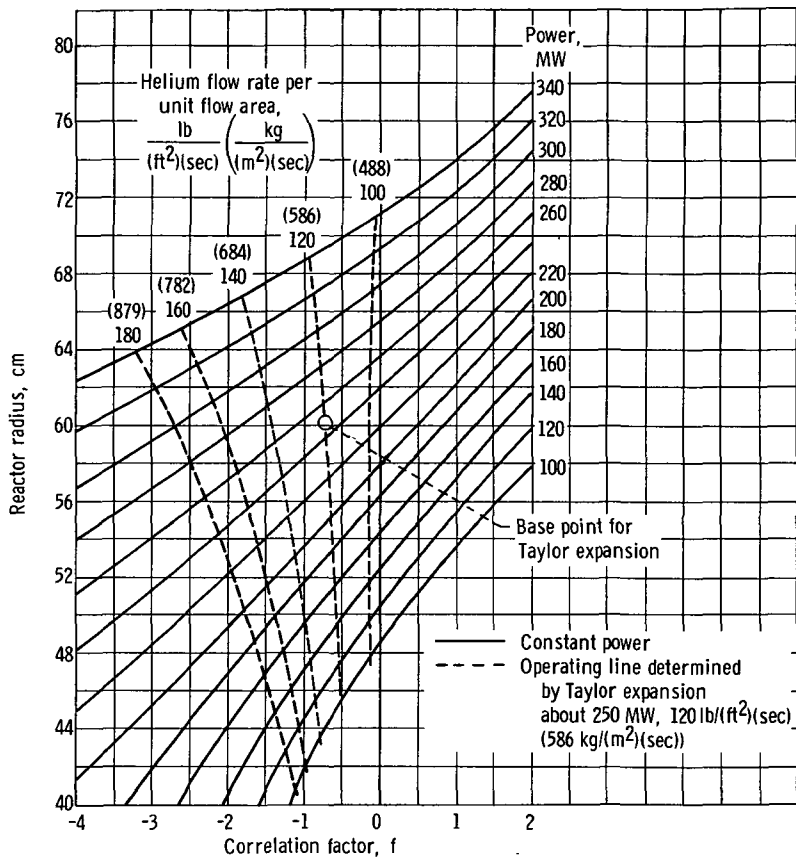
Figure 2. - Reactor radius against shield weight correlation factor for various power levels and weight flows per unit area. Helium inlet pressure, 1750 pounds per square inch (12.06x10⁶ N/m²); outlet temperature, 2360° R (1311 K); nominal maximum reactor wall temperature, 2560° R (1422 K).

sion given in appendix B provide a rapid means of estimating reactor performance. For this reason, the range of design cases presented is limited to values between 100 and about 400 megawatts.

Shield. - Shield weight is affected not only by the shield geometry and materials, but also by the size (and shape) of the reactor core for a given power level and how close the core or reflector can be to the first layer of shield material. Only unit shields are considered so that the airplane will not be activated to any extent that would limit operations or maintenance.

The unit shield weight calculations were made for a range of reactor power levels and f parameters for two general classes of materials. The calculations were for a dose rate of 2.5 millirem per hour at the nominal crew station (which varied with fuselage length) and included air scattering effects for sea level density. The base point shield is characterized as "currently buildable" and would be a relatively straightforward design using, essentially, various layers of metal and regions of water. The "ad-
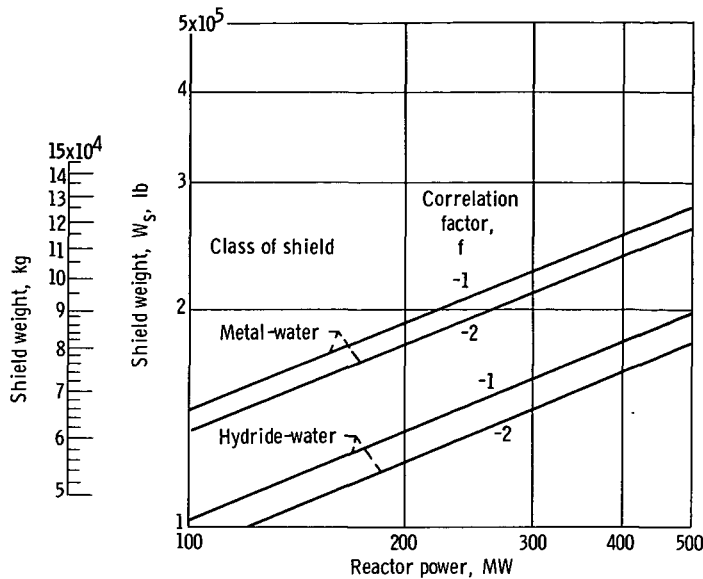
Figure 3. - Shield weight as function of reactor power.
Dose rate, 2.5 millirems per hour; distance, 130 feet
(39.6 m).

vanced'' shield materials would utilize layers of various metal hydrides and water; however, the chemical properties of the hydrides require special measures for protecting the shield units from water, air, and stress. The shields will be referred to as metal-water or hydride-water. The calculations were made using procedures called shield synthesis and Monte Carlo (SANE for neutron dose and SAGE for gamma ray dose, refs. 5 and 6). Examples of the variation of the unpenetrated unit shield weight with power level and factor f are shown in figure 3 and can be represented by the equation

$$W_s = (C_1 + C_2 f) \mathscr{P}^\beta \tag{1}$$

The parameters C_1 and C_2 depend on the shield materials, whereas the exponent β varied only slightly from a value of 0.406 to 0.419 for the ranges of conditions and materials considered (see appendix B). Over the power range of 100 to 500 megawatts, the effect of varying the core size parameter f from -1 to -2 was to increase the shield weight about 7 percent for the metal-water shield and about 9 percent for the hydride-water shield.

Shield packing factor and duct penetration: Additional considerations involve the penetration of the unit shield with the ducts containing the working fluid, helium, and the necessity of incorporating some equipment within the shield such as valves, motors, etc. For the latter item, the increased spacing between the core or reflectors and pressure vessel, or the placing of equipment within the shield material, increases the volume to

be covered by shield material. This is referred to herein as a "packing factor," and since it is really determined by detailed layout design, a simple percentage increase in shield weight is used in this design-point study.

Selection of a concentric helium duct for this analysis, such as that used in reference 3, allows a rather simple shield penetration. As shown schematically in figure 1, a half-turn helix within a certain bore diameter protects against direct neutron and gamma streaming, if some excess shield material is added beyond the original unit shield dimensions. The pressure drop and shield weight penalties associated with the dimensions of the half-turn helical duct penetration were optimized in a separate study. For the 1-million-pound (453 600-kg) airplane, the outside diameter of the concentric penetration duct was approximately 18 inches (0.46 m), with a bore or spiral diameter of about 4 feet (1.22 m).

Variation of shield weight with dose distance: Another shield weight variation is that due to dose distance as fuselage length to width ratio or gross weight is changed and dose rate maintained at a constant level. The relation used is

$$\frac{W_{s,D_d}}{W_{s,130}} = \frac{330 - 100 \log_{10} D_d}{118.6} \tag{2}$$

for D_d in feet or

$$\frac{278.4 - 100 \log_{10} D_d}{118.6} \tag{3}$$

where D_d equals $(130/264) \, l_f$ in feet or $(39.6/80.4) \, l_f$ in meters.

Heat exchanger and ducting. - The conceptual design of the helium to air heat exchanger, which was configured to fit between the compressor and chemical burner, was a four-pass cross-counter flow type. The tube bundle array (ref. 7) was constructed of four layers of 1/4-inch- (6.35×10^{-3}-m-) outside-diameter tubes with a nominal distance between headers of four feet (1.22 m). The tube-wall thickness, and hence internal tube diameter, was determined by a "thick tube" creep-rupture stress calculation based on the applied pressure and a tube-wall surface temperature determined by heat transfer. The stress-rupture equation for the material N155 for a creep-rupture life of 1000 hours at the surface temperature is

$$\sigma = 7000 \exp\left[-0.00447 \left(T_{wall,\,max} - 2060^{O}\,R\right)\right] \qquad psi$$

or

$$\sigma = 4825 \exp\left[-0.008046 \left(T_{wall,\,max} - 1144\,K\right)\right] \qquad N/m^2$$

(4)

where $T_{wall,\,max}$ is the maximum heat exchanger wall temperature.

The weight of the necessary tube bundle, headers, and inner and outer pressure shells was calculated and multiplied by a design stress safety factor of 10/7. The accompanying air and helium pressure drops were also determined. Since the primary component of the heat exchanger is the tube bundle, the main factors that determine the heat exchanger weight are the stress-rupture relation for the selected lifetime, the maximum tube-wall temperature, and the helium pressure. For a tube life expectancy of 10 000 hours, the front constant of equation (4) becomes 3800 for σ in psi or 2620 for σ in newtons per square meter.

The best procedure for manifolding the concentric helium lines from the separate engines prior to entering the shield has not been established. Therefore, a schedule of concentric duct length per engine was estimated from preliminary layouts as the routing distance from the shield to the middle engine. The values are given in table I.

A procedure for calculating the weight of the ducts was followed that resulted in the minimum duct weight for a given pressure drop and gas conditions. The total duct pressure drop includes terms for a nominal number of valves or bends.

Helium pump. - The power required to drive the helium pumps was extracted as shaft power from the engine cycle as shown in figure 1 and in equation (5):

$$\frac{\mathscr{P}_p}{\mathscr{P}} = \frac{\text{Pump power}}{\text{Total installed power}} = \frac{T_{in}}{\Delta T}\left[(PR)^{(\gamma-1)/\gamma\eta_p} - 1\right]$$

(5)

TABLE I. - SCHEDULE OF

DUCT LENGTH

Gross weight, W_g		ft/engine	m/engine
lb	kg		
0.5×10^6	0.227×10^6	30	9.15
.85	.386	42.5	12.95
1.0	.454	50	15.24
1.25	.567	60	18.28

The pressure ratio PR is for the complete system and composed of the heat exchanger, line, reactor, and shield pressure losses. The efficiency of the pump η_p was taken as 0.8. The weight of the pump and associated drive was estimated by means of

$$W_{pump} = \dot{w}_{He} \sqrt{T_{in}} \log_e(PR) + 0.0708\, C_{p,\,He}\, \Delta T \dot{w}_{He}$$

or (in SI units)

$$W_{pump} = 0.1086\, \dot{w}_{He} \sqrt{T_{in}} \log_e(PR) + 0.01784\, C_{p,\,He}\, \Delta T \dot{w}_{He}$$

(6)

Chemical (fossil) fuel allowance. - The chemical fuel used in flying the flight path to and from the cruise point and for emergency range was approximated by the procedure given in appendix C. For chemical operation during takeoff and climb, the turbine temperature was 2160° R (1200 K).

An emergency off-set range of 500 miles (804×10^3 m) was specified for all designs. This distance was the sum of the power-off glide range plus the remainder at cruise power conditions.

The actual mode of emergency flight may well differ from cruise conditions; however, this assumption at least provides a common first-order allowance varying with the airplane design points considered. No chemical fuel allowance for helium circulation during nonnuclear operations has been made due to the uncertainty at this time of the amount of circulation required.

Airplane Configuration and Operating Assumptions

The procedures adopted for estimating aircraft performance and weight represent a selection of existing methods configured to respond to the primary variables in this study; namely, design Mach number, altitude, and gross weight. The main items required from these programs are the drag and structural weight, so that the powerplant performance and its weight can be determined prior to obtaining the payload.

The general requirements for the airplane configuration include cargo volume, safety, air-drop ability, and landing speed. One version of a configuration that meets these needs is depicted in figure 4.

Some of the basic configuration assumptions were the following:

(1) The reactor-shield assembly would be mounted in the fuselage near the longitudinal center of gravity as high as possible (to give an unobstructed cargo bay).

(2) The landing gear would be completely fuselage mounted.
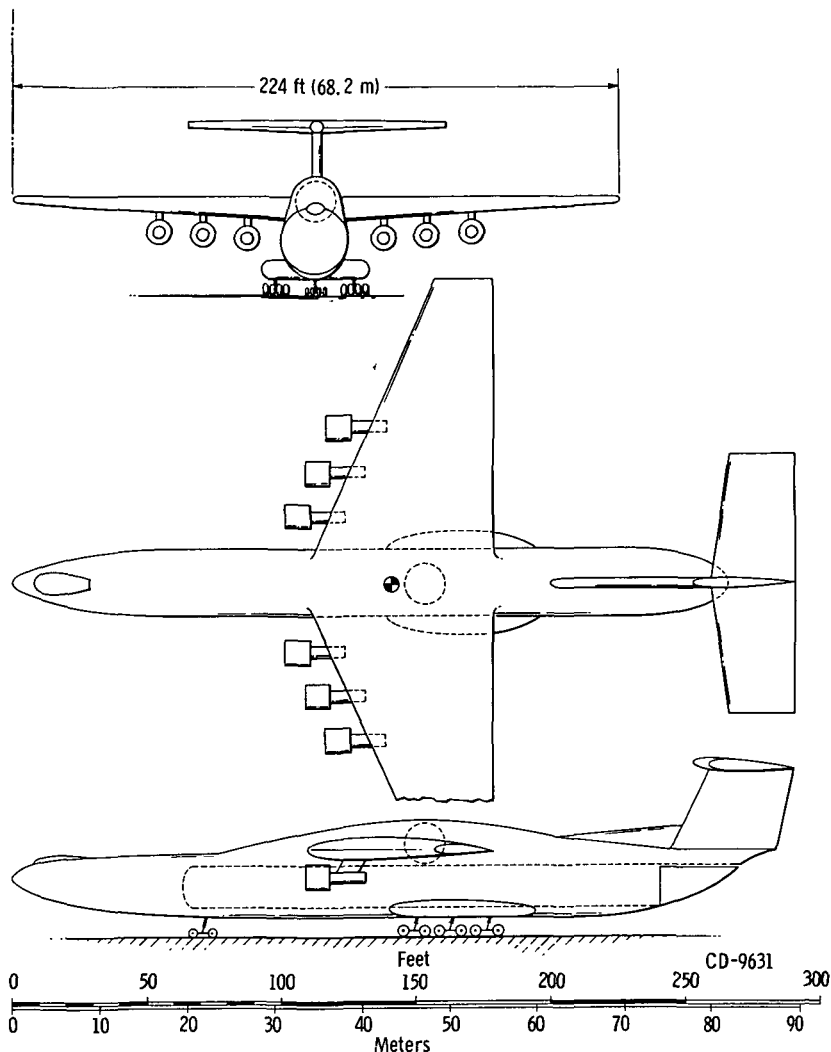
Figure 4. - Schematic of nuclear cruise, logistic airplane. Gross weight, 1×10^6 pounds; (453 600 kg) cruise Mach number, 0.8; cruise altitude, 36 089 feet (10 990 m).

(3) The longitudinal center of gravity was fixed at 55 percent of the fuselage length to give a large dose distance.

(4) A dorsal fin was used to help offset this rearward center of gravity.

(5) The wing was mounted above the cargo compartment and with the quarter chord of the mean aerodynamic chord alined with the center of gravity.

(6) The "T" tail was used to increase the tail moment arm and improve cargo handling.

(7) The engine pods, generally six, were mounted below the wing so that an externally blown, high-lift system could be used if necessary.

Airplane polar curve. - In order to determine the aircraft polar curve, knowledge of the profile drag and drag due to lift is necessary. More extensive details are given in appendix D, while sufficient background to accompany the results are given herein.
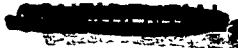
Profile drag: Because of the logistics role, a schedule of fuselage width with gross weight was established together with a general fuselage geometry (appendix D, eq. (D1)). The surface area of the fuselage group was compiled by summing the contributions from the basic body, the reactor-shield fairing, the sponsons for the landing gear, and the dorsal fin (appendix D, eq. (D2)). The fuselage group surface area only deviated from its dependence on gross weight due to small changes in reactor-shield size. The remaining surface areas, wing, tail, nacelles, and pylons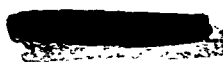 were determined within the optimization program to give the maximum payload for the given design Mach number, altitude, and gross weight. The maximum wing loading was restricted to a value compatible with a landing approach at 200 feet per second (61 m/sec) at a lift coefficient of 2.5. The wing thickness to chord ratio was constant at 0.18 up to $M_0 = 0.65$ and then decreased for higher Mach numbers (see appendix D, eq. (D3)). The wing sweepback angle at the quarter chord was a function of both flight Mach number and lift coefficient (appendix D, eq. (D4)). An additional wing geometry restriction was a planform taper ratio of 0.3. The horizontal and vertical tail areas were 25 and 10 percent, respectively, of the wing area. The surface area of the nacelles and pylons was formulated as a function of bypass ratio (appendix D, eq. (D5)).

The friction drag was calculated as the sum of the individual components based on the Reynolds number for a characteristic length of each and a roughness allowance of 0.0005 per unit wetted area. The method of reference 8 for turbulent compressible boundary layer was used. Additional corrections were made to the wing and tail profile drag as a function of thickness ratio (ref. 9).

Drag due to lift: The contribution of the wing to the drag due to lift was a function of aspect ratio, taper ratio, and sweepback angle. An arbitrary constant was assigned to correct for the variation of profile drag with lift (appendix D, eqs. (D8) and (D9)).

Structural weight estimation. - Although the methods employed for estimating structural weight are based on old construction techniques, such as skin-stringer, the magnitude of the answers agrees reasonably well with current predictions for very large airplanes. The structural procedures (appendix E) are functions of the same primary parameters used to configure the airplane and to compute the aerodynamics; therefore, the relative complexity is about equal for both the aerodynamics and weight procedures. The usual limit load factor of 2.5 was used.

Basically, the procedure calculates the weights of the wing and fuselage structures according to the applied loads after independent routines have been adopted for weight items such as fixed equipment and systems, landing gear, nacelles, and tail. The distribution of certain weight items is decided in advance. The nacelles and pylons, including engines, heat exchangers, pumps, and helium ducts, are assumed to be located within 30 percent of the semispan; whereas the chemical fuel is distributed over 90 percent of the semispan. The cargo, reactor and total shield (includes penetration altera-

tion), fixed equipment and systems, and landing gear, are located in the fuselage. The detailed equations are given in appendix E.

Engine size. - The installed thrust level at the design point was calculated by means of equation (7), which includes an arbitrary increment for a rate of climb potential of 300 feet per minute (91.5 m/min) as an allowance for maneuverability and hot days:

$$F_{inst} = C_D q_0 S_w + \frac{RC}{60} \frac{W_g}{V_0}$$

(7)

Generally, six engines were specified, unless the resulting sizes were unreasonable. Engine size was not adjusted for any uniform takeoff distance. Defining the operational limitations of nuclear aircraft is beyond the purpose of this report, and hence, the importance of runway length cannot be evaluated until such questions as special bases and overflying certain land areas have been resolved. However, the takeoff distance varied from a high of about 8000 feet (2438 m) for the design point M_0 of 0.4 and 20 000 feet (6096 m) in altitude to 5300 feet (1616 m) for an M_0 of 0.8 and 36 089 feet (11 000 m) in altitude.

Optimization Procedure

The purpose of the optimization routine was to define the combination of component performances that gave the maximum figure of merit, usually payload. The complete airplane design, including the nuclear system, the thermodynamic cycle analysis of the engine, and the aerodynamics and weight of the airplane, was determined by 12 independent variables. All other items were dependent or assigned parameters. The following independent variables were iterated until the maximum figure of merit was found for a selected design point (Mach number, altitude, and gross weight):

Engine:
    Fan pressure ratio
    Overall compressor pressure ratio
    Bypass ratio
    Heat exchanger air pressure drop
    Turbine inlet temperature
Nuclear system:
    Helium temperature out of reactor
    Helium temperature out of heat exchanger
    Helium heat exchanger pressure drop

Helium duct (line) pressure drop

Reactor helium weight flow rate per unit area

Airplane:

Cruise lift coefficient

Wing aspect ratio

Thus, the maximum payload obtained was not the result of independently optimizing the system components but, rather, the combination of component performance parameters that gave the best payload. For example, given the variation of the weight of some component with pressure drop, the lowest component weight would not be chosen because the accompanying high pressure drop would require more pump power, more installed reactor power, heavier shield, more drag, larger engines, etc. Some other self-consistent arrangement of independent and dependent variables could have been chosen. Further details and the flow chart for the optimizing procedure are given in appendix F.

RESULTS AND DISCUSSION

Explanation of Trade-offs for the Optimized System

The calculation procedure is arranged so that for a selected gross weight the primary items that are free to vary are wing area (and its associated geometry) and the magnitude of the installed power. As previously mentioned (see Profile drag, p. 18) the fuselage surface area is relatively fixed. Thus, as wing area, and hence its drag, changes, the installed power changes to provide the necessary thrust. Because the figure of merit is payload, the trade-off is primarily between the weight of the installed powerplant (which includes the items listed in System figure of merit and synthesis, p. 10) and the wing weight. Changes in fuselage weight are small compared with those for the wing; however, for a given size, the fuselage weight does reflect the loads applied by the body contents and the wing. For a selected design point and gross weight, the wing weight varies primarily with wing loading and aspect ratio. The powerplant weight is primarily determined by trading off the shield weight against the weights of the engines, heat exchangers, and chemical fuel. The smaller shield weights due to smaller reactor cores as produced by higher helium temperature rise and flow rates per unit area must be balanced against the effects of both the increased heat exchanger size and pumping power extracted from the engine cycle. Iterative corrections are made for a number of effects, such as nacelle-pylon drag and weight. The terminology "optimized system" as used hereinafter refers to the largest calculated payload that results for the combination of independent variables (listed under Optimization Procedure, p. 19) after

each has been separately perturbed in sequence numerous times (see appendix F). Exceptions to this terminology, such as fixing the value of an independent variable, are noted in the subsequent results and discussion. The maximum design temperature of the reactor wall was maintained at 2560° R (1422 K), the maximum helium temperature was 2360° R (1311 K), and, unless noted, the helium pressure (pump discharge) was 1750 psia (12.06×10^6 N/m^2).

Performance of the optimized system. - The performance calculated for an optimized system using metal-water shields with a packing factor of 1.33 for a range of gross weights from 1/2 to $1\frac{1}{4}$ million pounds (0.227×10^6 to 0.567×10^6 kg) and a flight spectrum from Mach 0.4 to Mach 0.8 at altitudes from 20 000 to 45 000 feet (6096 to 13 720 m) is presented in figures 5 to 7 and tables II and III. Results for the 1-million-pound (45.4×10^4-kg) airplane are shown in figure 5.

A payload fraction of 22.8 percent of the gross weight was obtained for a design altitude of 36 089 feet (11 000 m) at Mach 0.645 with only a small reduction (10 000 lb; 4536 kg) out to Mach 0.73 (fig. 5(a)).

At a design altitude of 20 000 feet (6096 m) the peak payload fraction increased to 26 percent at Mach 0.50, and decreased to about 15.5 percent at 45 000 feet (13 720 m) and Mach 0.675. These variations in payload are due to changes in powerplant and structural weight fractions (see tables II and III). These numerical results should be viewed as "gross" payload, inasmuch as various undefined penalties, such as crash hazard protection devices, are likely.

Converting these payload fractions to delivery rate (defined as the product of cargo weight and velocity), expressed as millions of ton-miles per hour (as in fig. 5(b)), shows that peak delivery rates occur at higher Mach numbers than peak payload, particularly for the 20 000-foot (6096-m) design case. The comparative peak magnitudes show an increase of 10 percent over the 36 089-foot (11 000-m) value for the 20 000-foot (6096 m) altitude, and a decrease of 32 percent for the 45 000-foot (13 720-m) design.

The wing loadings (at cruise) after the takeoff and climb chemical fuel has been consumed, the lift-drag ratios, and total engine stream tube area associated with the previous spectrum of design cases are shown in figure 5(c). (Wing loading is just another way of representing the independent variable, cruise lift coefficient.)

The results represent the balance between powerplant and structural weight fractions chosen by the optimizing procedure for maximum payload, as explained in the preceding section (Explanation of Trade-offs for the Optimizing System). The wing size was designed by the landing condition only for the 20 000-foot (6096-m) case at Mach numbers greater than about 0.525. For the other two altitude cases, the effects of sweepback angle on wing weight was offset by reverting to a lower wing loading and aspect ratio (see tables II and III) for Mach numbers greater than about 0.7.

This trend of decreased payload and optimum wing loadings between Mach 0.7 and

TABLE II. - MAJOR WEIGHT FRACTIONS AND GENERAL DESIGN PARAMETERS OF OPTIMIZED SYSTEM
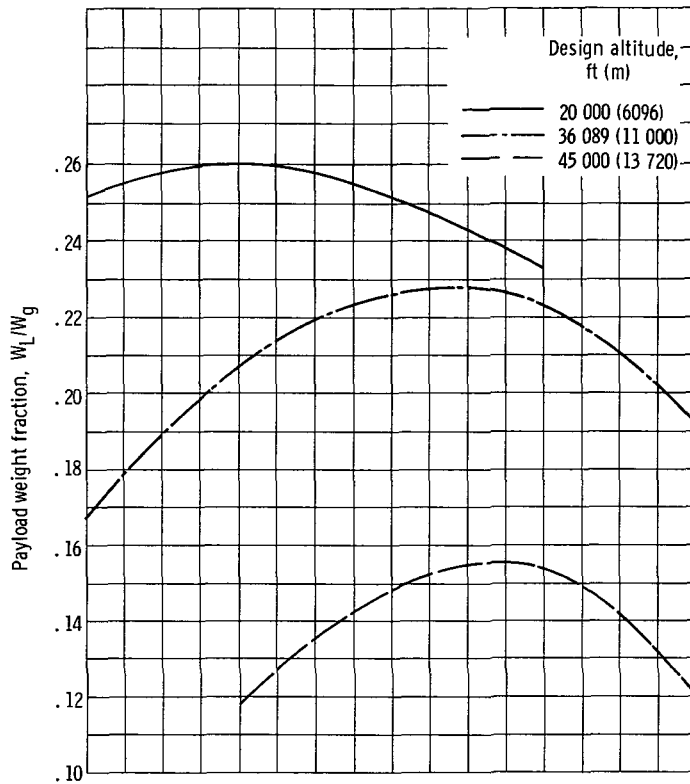
[Shield, metal-water with a packing factor of 4/3.]

| Design conditions					Major weight fractions										General					
W_g lb	W_g kg	H ft	H m	M_0	$\frac{W_L}{W_g}$	$\frac{W_{pp}}{W_o}$	$\frac{W_{str}}{W_g}$	$\frac{W_F}{W_g}$	$\frac{W_{s+p+rea}}{W_g}$	$\frac{W_{eng}}{W_g}$	$\frac{W_{HX}}{W_g}$	$\frac{W_{lines}}{W_g}$	$\frac{W_w}{W_g}$	$\frac{W_{fuse}}{W_g}$	$\mathscr{P}$, MW	$\frac{L}{D}$	W_g/S_w lb/ft²	W_g/S_w kg/m²	A_0 ft²	A_0 m²
1.0×10⁶	45.4×10⁴	20 000	6 096	0.4	0.252	0.367	0.381	0.065	0.215	0.038	0.034	0.013	0.131	0.132	188	17.3	75.7	370	451	41.9
				.5	.261	.379	.360	.064	.227	.037	.036	.014	.11	.133	224	17.15	109.4	534	350	32.5
				.6	.252	.403	.344	.068	.238	.039	.04	.016	.095	.133	279	16.3	118.9	580	283	26.3
				.7	.233	.441	.326	.082	.242	.046	.05	.017	.077	.132	384	14.0	118.9	580	258	24.0
1.0×10⁶	45.4×10⁴	36 089	11 000	0.4	0.168	0.399	0.433	0.082	0.207	0.064	0.034	0.011	0.184	0.126	175	17.1	44.1	215	700	65.0
				.5	.207	.393	.40	.07	.213	.06	.036	.012	.150	.129	188	17.4	59.5	290	556	51.6
				.6	.226	.395	.379	.065	.22	.057	.039	.012	.13	.13	209	17.5	81.3	397	440	40.9
				.7	.223	.407	.370	.064	.229	.055	.042	.015	.121	.130	240	17.1	99.3	485	404	37.5
				.8	.192	.441	.367	.073	.238	.063	.048	.015	.113	.134	309	14.94	85.2	416	368	34.2
1.0×10⁶	45.4×10⁴	45 000	13 720	0.5	0.118	0.440	0.443	0.0805	0.219	0.083	0.039	0.015	0.194	0.123	187	17.9	43.5	212	790	73.4
				.6	.148	.435	.417	.071	.225	.078	.044	.016	.169	.125	202	18.3	58.6	286	606	56.3
				.7	.154	.442	.403	.0685	.230	.075	.052	.015	.157	.126	226	18.12	68.2	333	473	43.9
				.8	.1195	.479	.401	.078	.235	.091	.056	.016	.146	.131	291	15.71	58.4	285	507	47.1
0.5×10⁶	22.7×10⁴	36 089	11 000	0.8	0.05	0.585	0.365	0.062	0.407	0.059	0.045	0.011	0.115	0.135	127	16.0	93.6	457	184	17.1
.85	38.6	→	→	.8	.170	.464	.365	.067	.272	.062	.048	.013	.116	.132	237	15.4	87.2	426	336	31.2
1.25	56.7			.8	.218	.398	.385	.075	.189	.064	.049	.018	.120	.14	396	14.9	84.0	410	503	46.7
.5	22.7			.6	.109	.519	.372	.057	.367	.055	.029	.011	.126	.131	90.3	18.8	86.9	424	220	20.4
1.25	56.7			.6	.241	.367	.392	.07	.181	.060	.039	.015	.131	.136	282	16.9	80.7	394	663	61.6

TABLE III. - INDEPENDENT VARIABLES AND RELATED PARAMETERS OF OPTIMIZING SYSTEM

[Shield, metal-water with a packing factor of 4/3.]

| Design conditions					Engine cycle											Nuclear system								Airplane				
W_g		H		M_0	$\frac{P_2}{P_1}$	$\frac{P_3}{P_1}$	BPR	T_4		$F/\dot{w}_a$		η_{oa}	$\frac{\Delta P_{3-4a}}{P_3}$	T_{ex}		$T_{HX,out}$		$\frac{\Delta P}{P_{He}}\big|_{total}$	$\frac{\Delta P_{HX}}{P_{He}}$	$\frac{\mathscr{P}_p}{\mathscr{P}}$	$\dot{w}_{He}/A$		$\frac{\Delta P_{rea}}{P_{He}}$	C_L	AR	$C_{D,o}$	$C_{D,1}$	$C_{D,total}$
lb	kg	ft	m					°R	K	lb/(sec)	N/(kg)(sec)			°R	K	°R	K				lb/(ft²)(sec)	kg/(m²)(sec)				100	100	100
1.0×10⁶	45.4×10⁴	20 000	6 096	0.4	1.24	19.00	8.40	1980	1100	9.06	88.8	0.206	0.093	2360	1311	1407	782	0.070	0.0065	0.058	137.6	672	0.042	0.695	7.08	1.53	2.49	4.02
				.5	1.28	16.64	6.56	1950	1083	9.1	89.2	.21	.100	→	→	1396	776	.082	.0062	.067	147.3	719	.049	.643	7.40	1.70	2.05	3.75
				.6	1.31	14.30	4.61	1885	1047	9.52	93.4	.206	.094	→	→	1363	757	.103	.0066	.082	164.0	801	.062	.485	6.70	1.70	1.27	2.97
				.7	1.34	14.50	2.92	1845	1025	10.13	99.4	.196	.114			1284	713	.142	.0086	.104	179.9	879	.076	.356	4.79	1.62	.93	2.54
1.0×10⁶	45.4×10⁴	38 089	11 000	0.4	1.33	20.15	7.77	1928	1071	11.14	109.3	0.207	0.106	2360	1311	1358	754	0.075	0.0053	0.056	147.0	718	0.049	0.831	7.40	1.43	3.43	4.86
				.5	1.36	21.00	6.98	1944	1080	10.73	105.3	.230	.108	→	→	1364	758	.075	.0060	.057	146.0	713	.048	.718	7.16	1.49	2.63	4.13
				.6	1.41	20.20	5.69	1939	1077	11.00	107.9	.241	.107	→	→	1368	760	.083	.0062	.065	150.2	734	.051	.681	7.47	1.60	1.29	3.89
				.7	1.41	19.12	5.52	1981	1100	10.32	101.2	.245	.114			1423	791	.095	.0076	.084	157.0	767	.055	.610	7.06	1.64	1.93	3.57
				.8	1.46	18.43	3.61	1890	1050	11.07	108.6	.242	.121			1320	733	.124	.0080	.095	179.2	875	.075	.401	4.69	1.45	1.24	2.69
1.0×10⁶	45.4×10⁴	45 000	13 720	0.5	1.38	18.84	7.55	2038	1132	11.16	109.4	0.222	0.109	2360	1311	1563	868	0.062	0.0045	0.068	122.3	597	0.030	0.803	7.96	1.47	3.01	4.84
				.6	1.45	20.00	6.29	2076	1153	11.66	114.3	.237	.114	→	→	1564	869	.069	.0054	.077	125.1	611	.032	.752	8.25	1.55	2.55	4.10
				.7	1.56	18.82	4.84	2068	1149	12.73	124.8	.245	.119	→	→	1481	823	.082	.0070	.079	139.6	682	.042	.643	7.48	1.52	2.03	3.55
				.8	1.51	20.00	3.36	1907	1059	11.65	114.2	.243	.123			1348	749	.121	.0067	.096	179.2	875	.075	.422	4.90	1.36	1.32	2.68
0.5×10⁶	22.7×10⁴	38 089	11 000	0.8	1.44	20.30	4.76	1939	1077	10.40	102.0	0.277	0.100	2360	1311	1415	786	0.067	0.0057	0.055	147.8	722	0.049	0.441	6.40	1.62	1.14	2.76
.85	38.6		→	.8	1.43	20.30	4.53	1924	1069	10.00	98.1	.261	.105	2360	1311	1358	754	.100	.0067	.078	169.0	825	.066	.411	5.19	1.48	1.19	2.67
1.25	56.7			.8	1.40	18.30	3.80	1867	1037	10.10	99.1	.236	.117	2352	1307	1287	715	.141	.0075	.105	173.6	848	.069	.396	4.61	1.43	1.22	2.65
.5	22.7			.6	1.38	20.50	6.70	1937	1076	10.40	102.0	.263	.091	2192	1218	1526	848	.029	.0040	.035	120.1	586	.015	.728	9.67	1.78	2.10	3.90
1.25	56.7			.6	1.33	20.10	6.25	1911	1062	9.42	92.4	.230	.112	2360	1311	1323	735	.114	.0077	.085	171.7	839	.069	.676	6.93	1.60	2.40	4.00

(a) Payload.
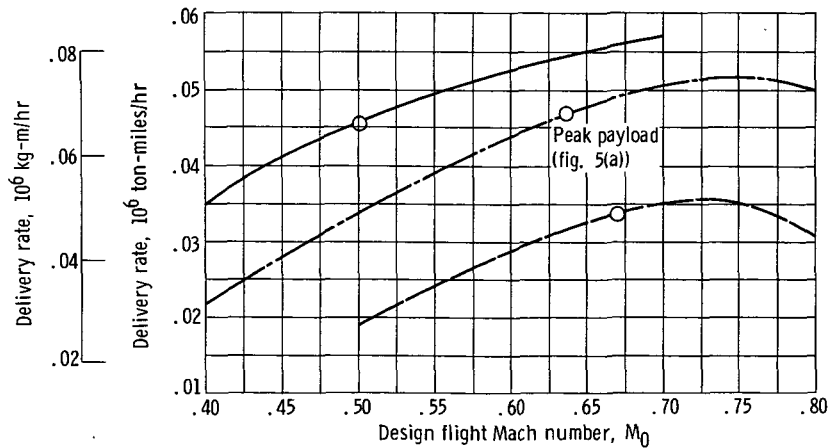
(b) Delivery rate.

Figure 5. – Performance of the optimized system. Gross weight, 1×10^6 pounds (453 600 kg); shield, metal-water with packing factor of 4/3.
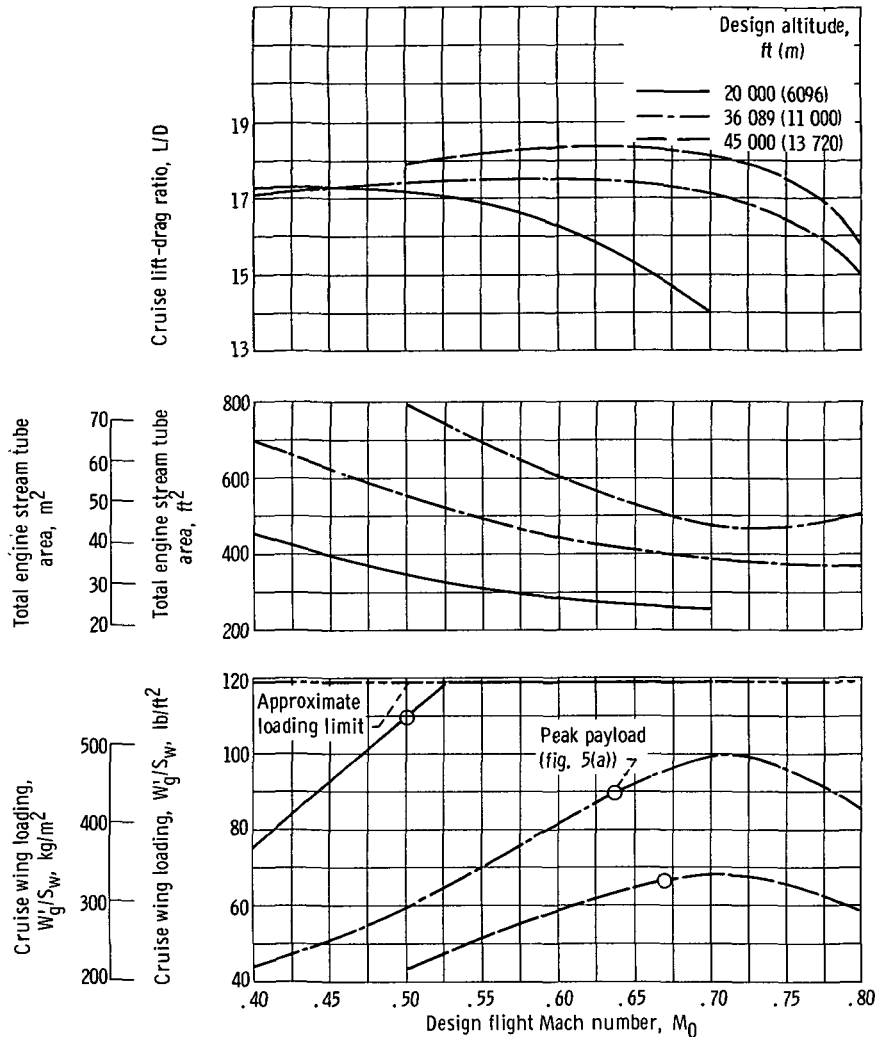
(c) Wing loading, engine area, and lift-drag ratio.

Figure 5. - Concluded.

0. 8 was investigated at the design altitude of 36 089 feet (11 000 m). The payload decrease (0.22 to 0.19) was mainly the result of an increase in powerplant weight, since the structural weight changed very little. The lift-drag ratio (tables II and III) decreased from about 17 to 15, which corresponded to an 11-percent drag increase. Although the total drag coefficient decreased 25 percent, mostly because of lower drag due to lift, the product of dynamic pressure and wing area $q_0 S_w$ increased 50 percent, mostly due to Mach number, and thus resulted in the previously quoted drag increase. Similar reasoning should apply to the 45 000-foot (13 720-m) case.

Calculations over a broad range of off-optimum wing loadings at Mach 0. 8 from 60 to 119 pounds per square foot (287. 2 to 578. 5 kg/m^2) showed that the payload was, indeed, maximum for the indicated optimum wing loading of 85. 2 (408 kg/m^2) (cruise lift

coefficient of 0.401). For the specified fixed conditions (W_g, M_0, H, C_L), the weights of the powerplant and wing are related through aspect ratio but not in a simple or direct manner. Thus, in effect, aspect ratio was varied by the optimizing procedure to find the value that gave the best payload (the other independent variables were free to seek new values if profitable).

These results should be considered preliminary since additional considerations of a more detailed nature, for example, wing flutter, may alter the trade-offs or add other boundaries.

The cruise lift-drag ratios for the spectrum of design cases were as high as 18.3, but decreased to between 16 and 14 for the highest Mach number considered for each altitude. The Mach number for maximum payload, figure 5(c), did not correlate with maximum lift-drag ratio or wing loading.

The total stream tube areas are presented in figure 5(c) primarily to illustrate the variation of design-point engine airflow requirements. Furthermore, if a velocity ratio of 1.0 is selected between the stream and the blading (V_1/V_0), a fan diameter can be estimated. For a six engine airplane, the largest area corresponds to a fan diameter of about 13 feet (3.96 m) and the smallest is about 7.4 feet (2.25 m). This estimate of fan diameter only affects the calculated results by way of the nacelle weight and drag which are a very small fraction of the total drag and structural weight (appendixes D and E).

Some other very general trends can be observed from the data of tables II and III. The installed power varied from about 175 to 384 megawatts, of which from 5 to as much as 10.4 percent was needed for helium pump power. For the engine cycle parameters the overall compressor pressure ratio was between 14 and 21, and it generally reached a peak at some intermediate value of Mach number. Fan pressure ratio increased with flight Mach number and altitude, and was within the range 1.2 to 1.6. Bypass ratio varied between 8.4 and 2.9, and decreased with increasing Mach number as cycle efficiency increased. Turbine inlet temperatures were in the range 1800° to 2100° R (1000 to 1166 K), and they generally were higher at the highest altitude.

Since airplanes designed for altitude extremes such as 20 000 or 45 000 feet (6096 or 13 720 m) may be operationally limited, an altitude of 36 089 feet (11 000 m) was selected for the remainder of this study. For example, the usual "over-weather" criterion requires an altitude capability of at least 30 000 feet (9140 m), and flight at an altitude of 45 000 feet (13 720 m) is no advantage for logistic missions. A Mach number of 0.8 was also selected as a base point, when necessary, since most advanced subsonic cargo planes fly at or near this speed.

Effect of gross weight. - Payload fraction increases with gross weight at a decreasing rate for either Mach 0.6 or 0.8, as shown in figure 6. This occurs because the decrease in powerplant weight fraction with gross weight has leveled out and the structural fraction increased a few percent of gross weight at the higher gross weights. Delivery
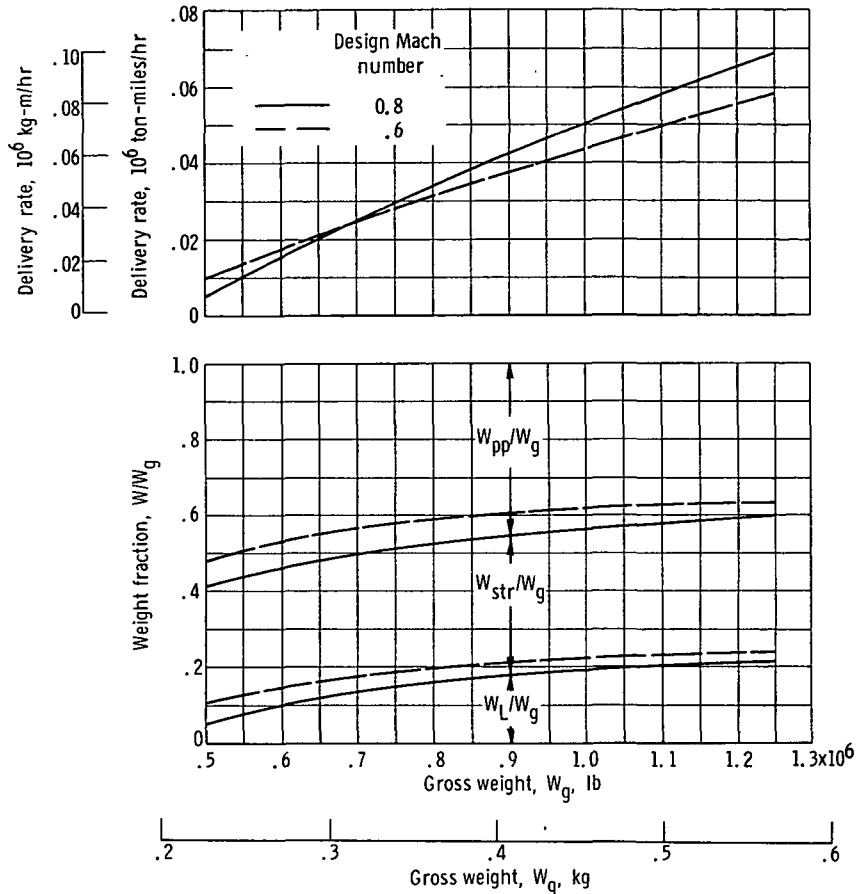
Figure 6. - Variation of weight fraction and delivery rate with gross weight for the optimized system. Design altitude, 36 089 feet (11 000 m); shield, metal-water with packing factor of 4/3.

rate also increases monotonically with gross weight. The magnitude of the payload for the 1/2-million-pound (22. 7×10^4-kg) airplane is one-eighth of that for the 1-million-pound (45. 4×10^4-kg) aircraft. Again, these trends are representative of the parametric families and technology level used. The transition from preliminary to detailed or layout design may reveal exceptions or alternates to the rules employed; for example, new materials (such as composites) and structural techniques may favor large aircraft. The variation of the weights of components of the powerplant and structural groups with aircraft gross weight is presented in figure 7 for the base-point conditions for the optimized system at Mach 0. 8 and 36 089 feet (11 000 m). Of particular interest as gross weight increases is the counteracting effect between the favorable decrease in shield weight (including duct penetration) fraction (W_{s+p}/W_g = 0. 39 to 0. 17) and the increase in the chemical fuel, engines, heat exchangers, and lines. The sum of these latter items increased from W_{SUM}/W_g = 0. 18 to 0. 22 and thus represents an important weight group. For the lower gross weight, the shield weight fraction is proportionally greater (than for
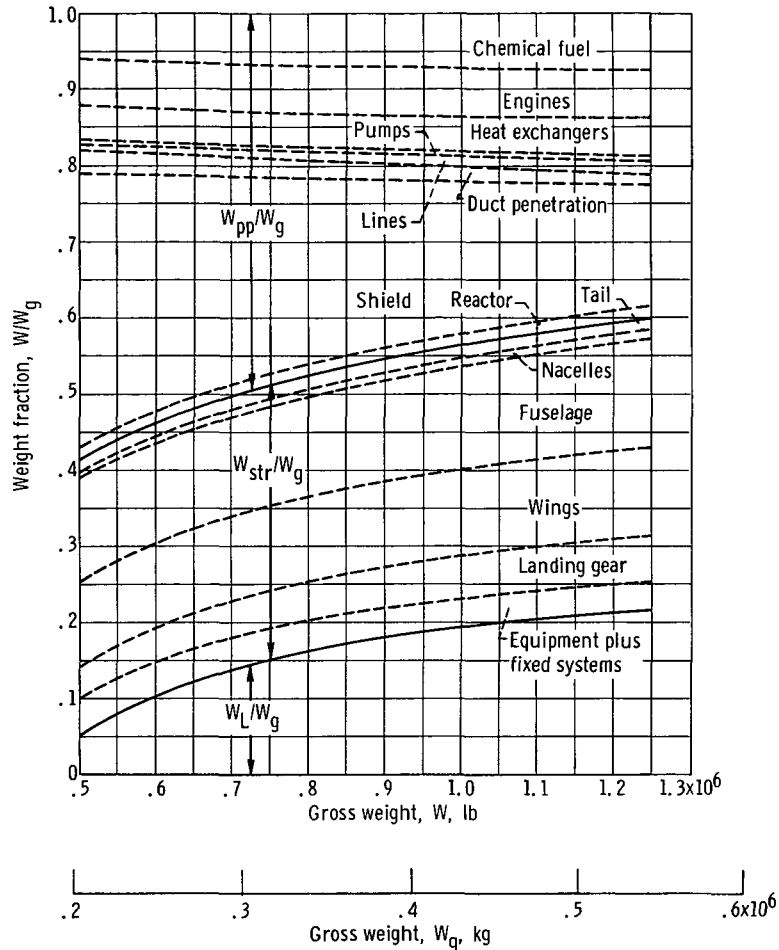
Figure 7. - Detailed weight breakdown as function of gross weight. Design flight Mach number, 0.8; altitude, 36 089 feet (11 000 m); shield, metal-water with packing factor of 4/3.

higher W_g's) not only due to the lower installed power (eq. (1)), but also due to the decreased dose distance (eq. (2)) and the constant dose level criterion.

The relative percentages of the weights of various items in the structural group (such as wing, fuselage, and tail) were also relatively constant over the range of gross weights (fig. 7) except for those items specifically programmed as functions of gross weight (such as the fixed equipment and systems, and landing gear).

The reason for the chemical fuel fraction increasing with gross weight is related to the general decline of engine efficiency and lift-drag ratio (as W_g increases). Again, the trade-off is between installed power and wing area as given in the previous section. However, because the power changes with gross weight the program seeks a balance between the shield weight as affected by reactor flow rate $\dot{w}_{He}/A$ and helium temperature rise (different relative core size) which, in turn, varies the helium pressure drop and

hence pump power requirements. Extracting pump power from the engine cycle changes the overall engine efficiency and, therefore, alters the chemical fuel allowance. The engine efficiency during chemical operation, which is without pump power extraction, is higher than during nuclear operation, but follows the trend for the nuclear operation since the cycle parameters are optimized for the nuclear cruise condition.

The lift-drag ratio varies (slightly) as a result of obtaining the best balance between wing weight (size and geometry) and powerplant weight for maximum payload.

Effect of engine type. - The optimum propulsive system defined in the preceding results, wherein bypass ratio was one of the twelve independent variables, was in all cases a turbofan. A comparison of the performance and nominal values of certain cycle parameters for the optimized system using turbofan (BPR > 0) or turbojet (BPR = 0) engines is shown in figures 8 and 9. The advantage for turbofan propulsion in terms of payload fraction varied from about 16 percent improvement at Mach 0.8 to almost
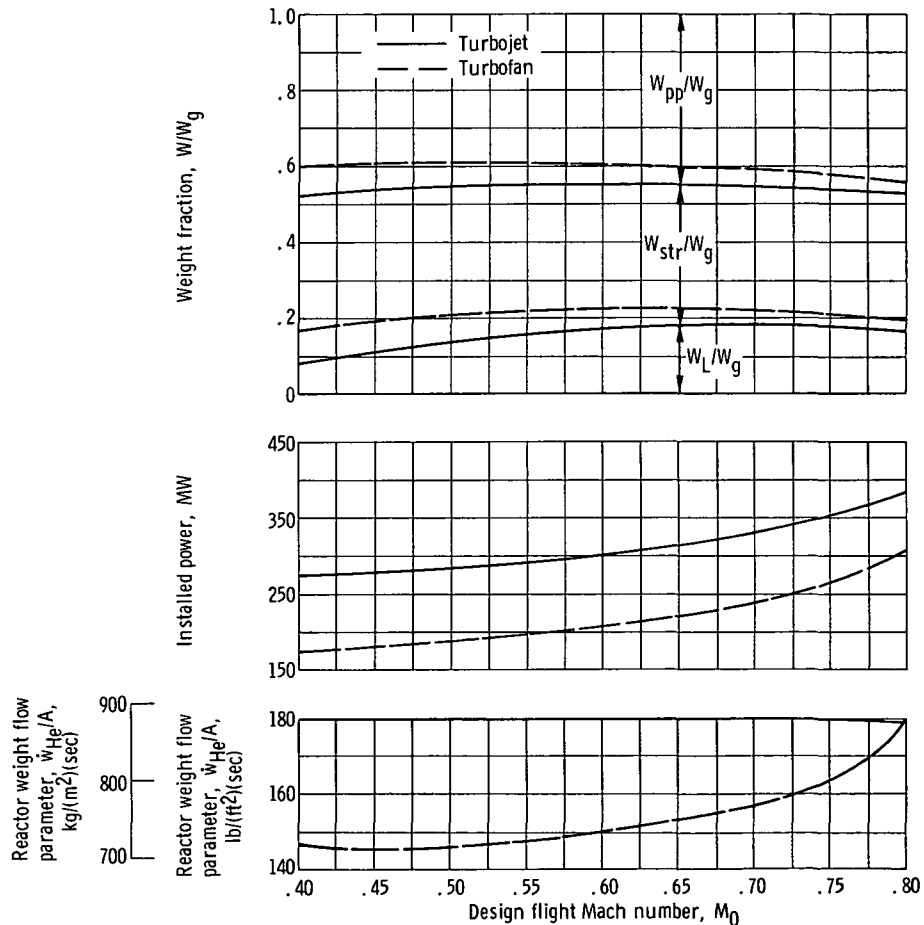
Figure 8. - Comparison of turbojet and turbofan propulsion for optimized system. Gross weight, 1 million pounds (453 600 kg); altitude, 36 089 feet; (11 000 m) shield, metal-water with packing factor of 4/3.
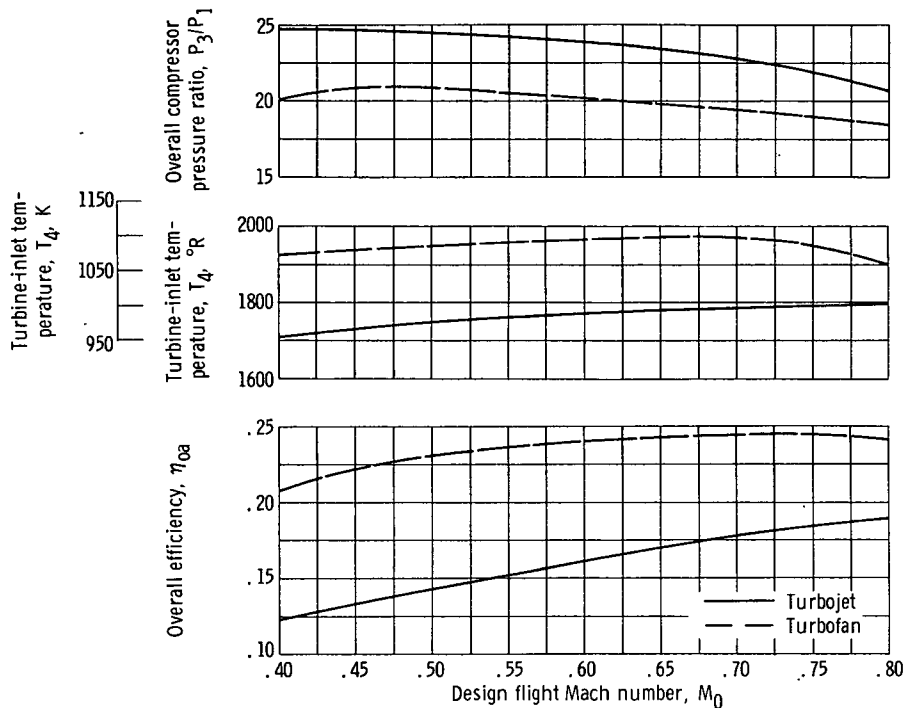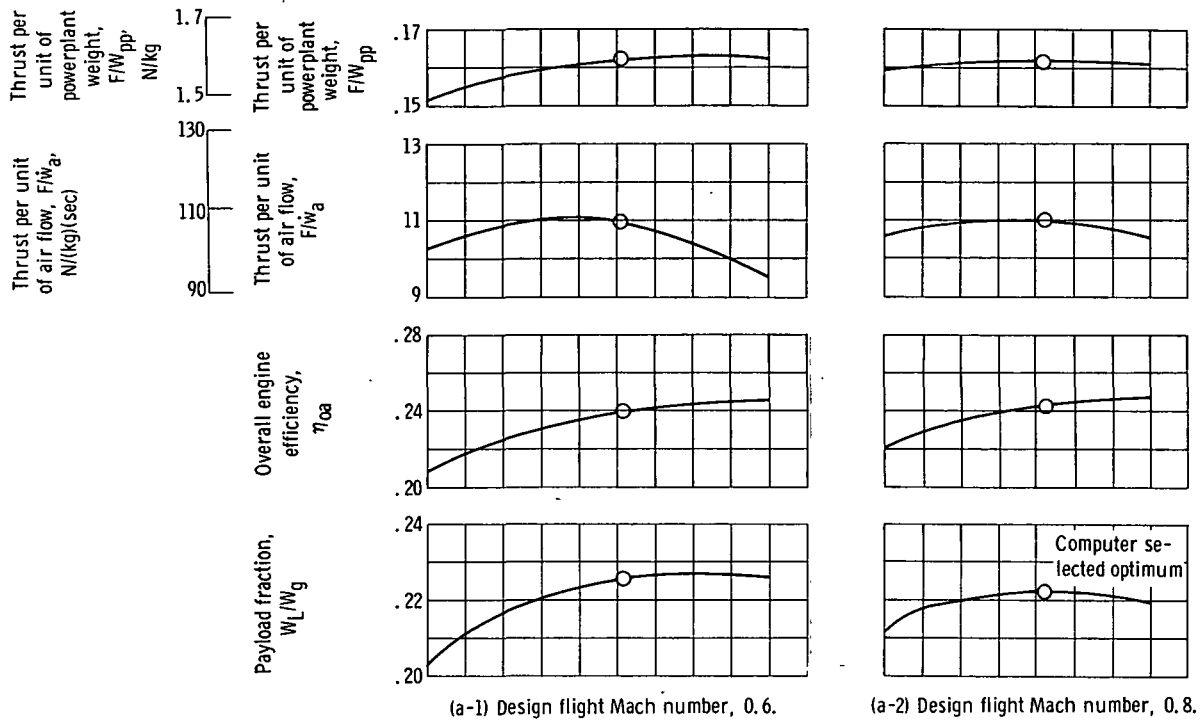
29

Figure 9. - Comparison of turbojet and turbofan cycle parameters for optimized system. Gross weight, 1 million pounds (453 600 kg); altitude, 36 089 feet (11 000 m); shield, metal-water with packing factor of 4/3.

108 percent at Mach 0. 4. This is primarily related to the inherent higher overall efficiency of the turbofan cycle at lower Mach numbers. The fan cycle was nearly twice as efficient as the jet cycle at this low speed condition and was 5 to 8 efficiency counts higher over the range of Mach numbers (fig. 9). The jet cycle attempts to counter this effect of lower overall efficiency by seeking higher cycle pressure ratios but is tempered by the effect of increasing engine weight. The fan cycle favors higher turbine inlet temperatures primarily because of the need for turbine power to drive the fan.
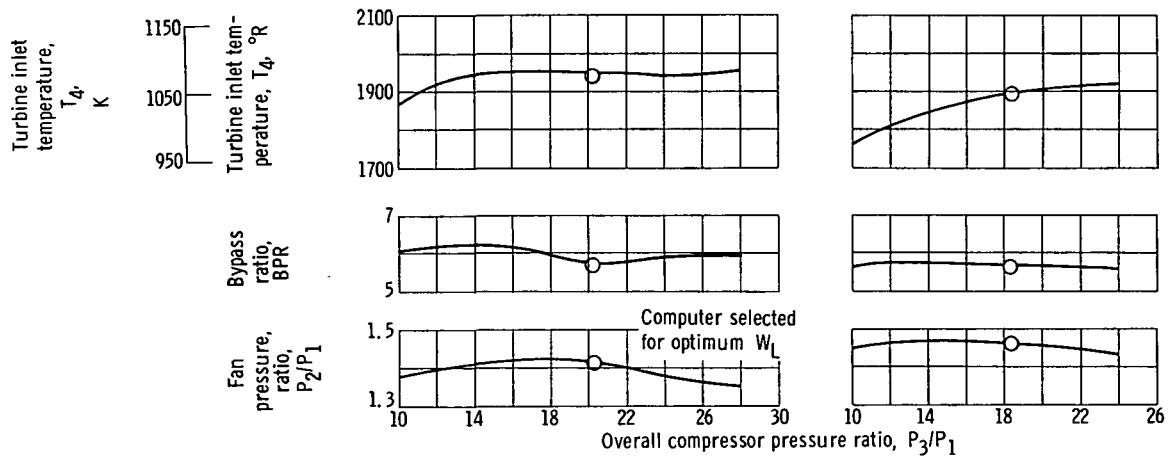
Effect of Off-Optimum Component Performance

Two general types of component performance variations are classified herein. The first type considers large changes such as advances in technology or major alterations of initial goals. The second type referred to as sensitivity factors is for smaller increments of the component performance such as may occur during detailed design.

Effect of overall compressor pressure ratio. - The importance of overall compressor pressure ratio to payload and the accompanying values of various other parameters are shown in figure 10 for the 1-million-pound (45.4×10^4-kg) airplane at Mach 0. 6 and

Thrust per unit of powerplant weight, F/W_{pp}, N/kg

1.7

1.5

Thrust per unit of air flow, $F/\dot{w}_a$, N/(kg)(sec)

130

110

90

Turbine inlet temperature, T_4, K

1150

1050

950

Thrust per unit of powerplant weight, F/W_{pp}

.17

.15

Thrust per unit of air flow, $F/\dot{w}_a$

13

11

9

Overall engine efficiency, η_{oa}

.28

.24

.20

Payload fraction, W_L/W_g

.24

.22

.20

Computer se-lected optimum

(a-1) Design flight Mach number, 0.6.   (a-2) Design flight Mach number, 0.8.

(a) Payload and some engine related dependent variables.

Turbine inlet temperature, T_4, °R

2100

1900

1700

Bypass ratio, BPR

7

5

Fan pressure ratio, P_2/P_1

1.5

1.3

Computer selected for optimum W_L

10   14   18   22   26   30   10   14   18   22   26
Overall compressor pressure ratio, P_3/P_1

(b-1) Design flight Mach number, 0.6.   (b-2) Design flight Mach number, 0.8.

(b) Engine dependent variables.

Figure 10. - Effect of overall compressor pressure ratio. Gross weight, 1 million pounds (453 600 kg); altitude, 36 089 feet (11 000 m); shield, metal-water with packing factor of 4/3.

0. 8.   The optimum overall pressure ratios which varied with flight design point have been presented in tables II and III.

Overall compressor pressure ratio affects payload primarily through the weight of the installed powerplant.   The installed power varies inversely with the overall efficiency as shown by

$$\mathscr{P} \propto \frac{V_0 W_g}{\frac{L}{D} \eta_{oa}} \propto \frac{V_0 \frac{F}{\dot{w}_a} \dot{w}_a}{\eta_{oa}} \tag{8}$$

In appendix A, the engine weight is given as a function of overall pressure ratio, bypass ratio, turbine temperature, and thrust.   This, together with equation (8), illus-
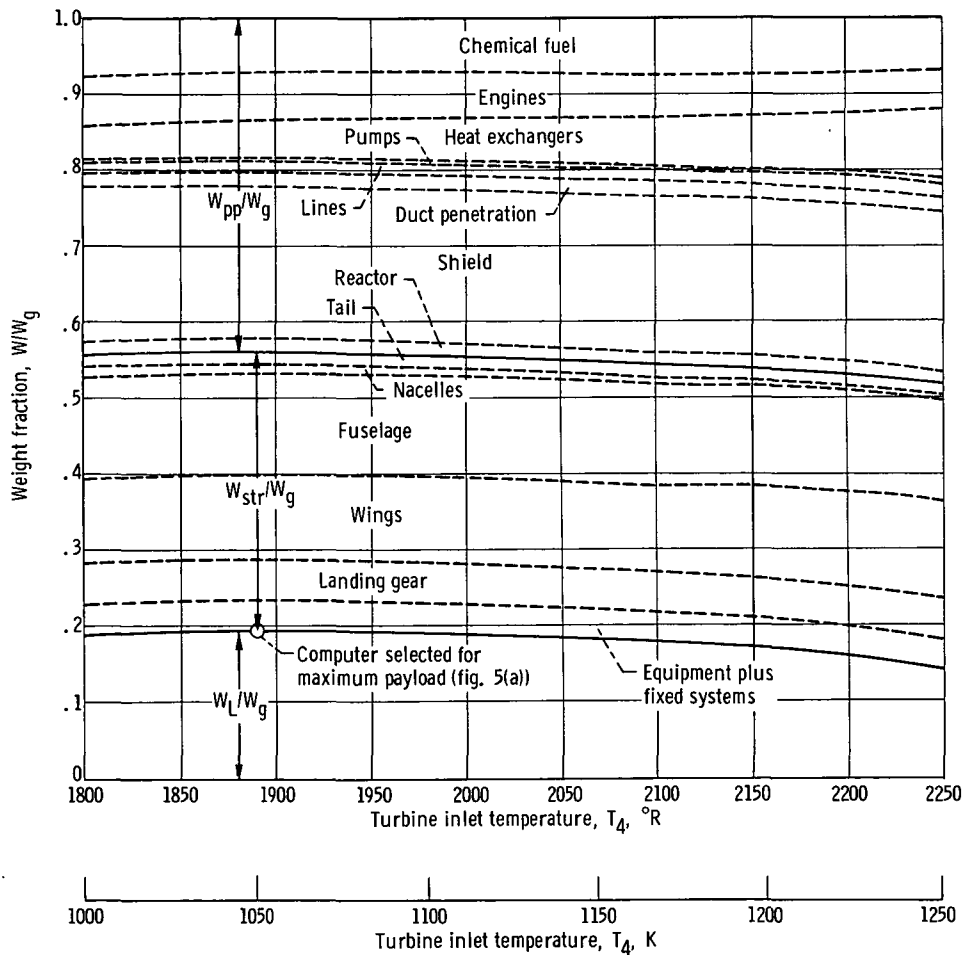
Figure 11. - Effect of turbine inlet temperature on weight distribution. Gross weight, 1 million pounds (453 600 kg); design Mach number, 0.8; altitude, 36 089 feet (11 000 m); shield, metal-water with packing factor of 4/3.
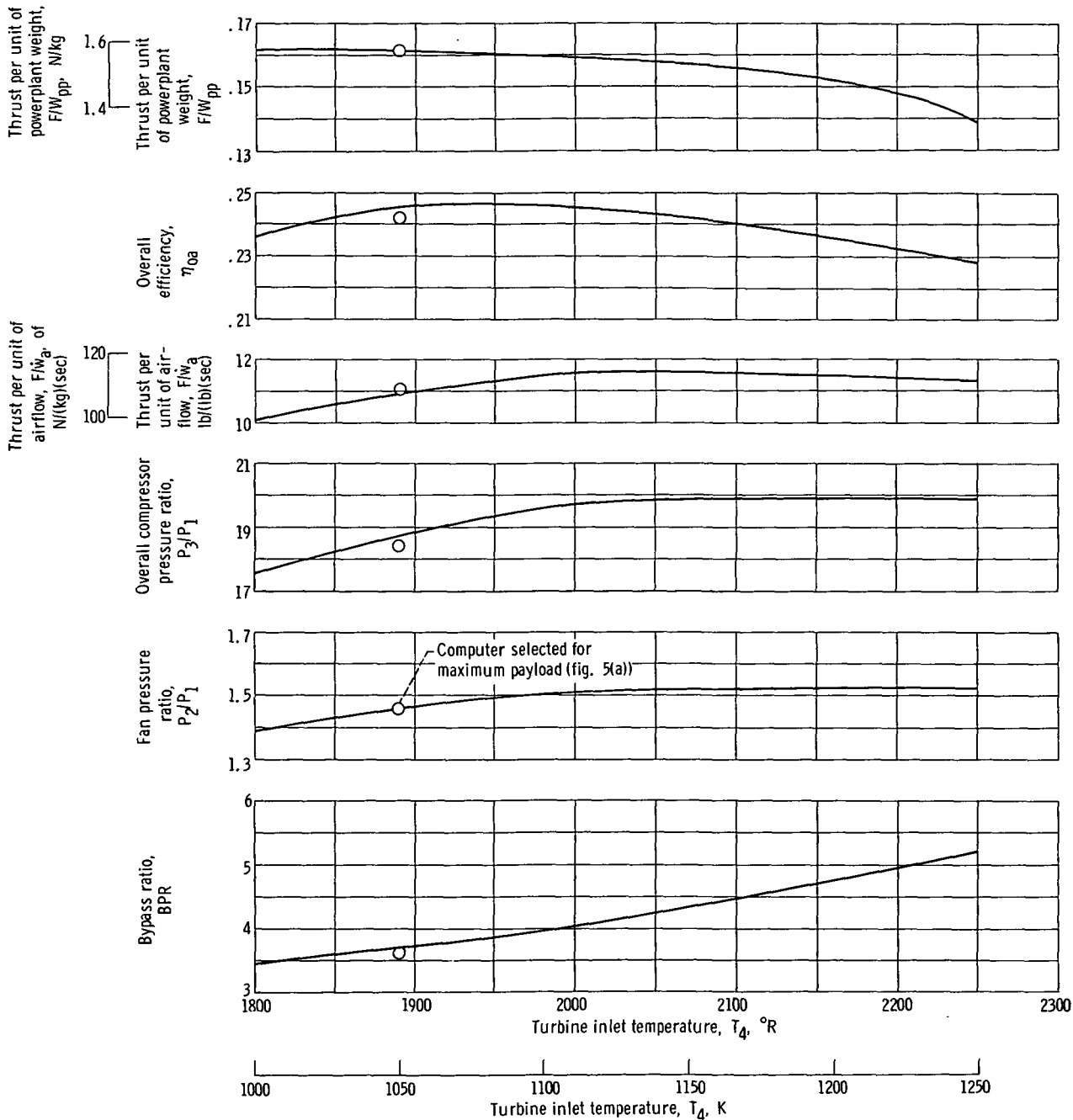
Figure 12. - Variation of engine characteristics with turbine inlet temperature. Gross weight, 1 million pounds (453 600 kg); design Mach number, 0.8; altitude, 36 089 feet (11 000 m); shield, metal-water with packing factor of 4/3.

TABLE IV. - EFFECT OF HIGHER THAN OPTIMUM TURBINE

INLET TEMPERATURE FOR BASE-POINT CONFIGURATION

	Turbine inlet temperature, T_4		Percent change
	[a]1890° R (1049 K)	2250° R (1249 K)	
Weight fraction			
Heat exchanger	0.048	0.0922	92
Engine	.063	.050	-20
Ducts	.015	.020	33
Payload	.192	.145	-25

[a]This temperature corresponds to maximum W_L/W_g.

trates the trade-off between shield weight (function of $\mathscr{P}$, eq. (1)) and engine weight for maximum payload as overall compressor pressure ratio is varied. Values of the other independent variables for the engine that corresponded to maximum payload for a pre-scribed overall compressor pressure ratio are shown in figure 10(b).

The symbol representing the "computer selected" independent variable values for best payload do not always lie on the faired lines of parametric values. This small dis-crepancy represents a band of alternate selection within which the independent variables may be mutually traded without altering the payload (within its convergence tolerance).

Effect of turbine temperature. - The effect on payload fraction and some engine cycle parameters of varying the turbine inlet temperature over the range 1800° to 2250° R (1000 to 1249 K) is shown in figures 11 and 12. The nominal maximum reactor wall temperature was 2560° R (1422 K) and the temperature of the helium leaving the reactor was not permitted to exceed 2360° R (1311 K). Because of the freedom to re-optimize other components, the payload fraction varied only 7 percent over the range of turbine temperature of 1800° to 2100° R (1000 to 1166 K), but was 25 percent below the maximum at 2250° R (1249 K). The peak payload value occurred at 1890° R (1049 K). At the higher temperatures, the heat exchanger weight increased more than the engine weight decreased as shown in the powerplant weight breakdown and in table IV. For the lower turbine temperatures, the cycle parameters are generally reduced due to the dif-ficulty of maintaining a positive work out of the turbine.

The small payload penalty for the lower turbine inlet temperatures suggests that lower reactor wall and helium temperatures, having simpler materials problems, may give comparable results.

Effect of heat exchanger pressure drop and lifetime. - The heat exchanger is the in-terface between the helium and air sides of the system. Once the heat exchanger is pro-portioned to transfer the required energy to the air, the resulting air-side pressure drop, although the magnitude is important to the cycle performance, assumes an almost

constant value of 10 percent (table II) (includes burner pressure loss) and is apparently not strongly affected by the feedback effect of engine weight on the helium-side weight. An air-side pressure drop of this magnitude causes about a 10-percent reduction in overall efficiency η_{oa}.

Extending the calculated lifetime of the heat exchanger from 1000 to 10 000 hours had a very small effect on payload. Heat exchanger weight increased 9250 pounds (4195 kg), or 19 percent, and payload decreased about 9800 pounds (4443 kg), or 5.1 percent, for the base-point configuration (M_0 = 0.8, altitude = 36 089 ft (10 990 m), $W_g/10^6$ = 1.0 lb (0.4536 kg), φ = 4/3).

<u>Effect of system pressures</u>. - The effect of changing the helium pressure from the value of 1750 psia (12.06×10^6 N/m^2) thus far considered is shown in figure 13. No maximum was found within the range from 1600 to 2000 psia (11.03 to 13.8×10^6 N/m^2), and the increase in payload over the range was only 1.5 percent.
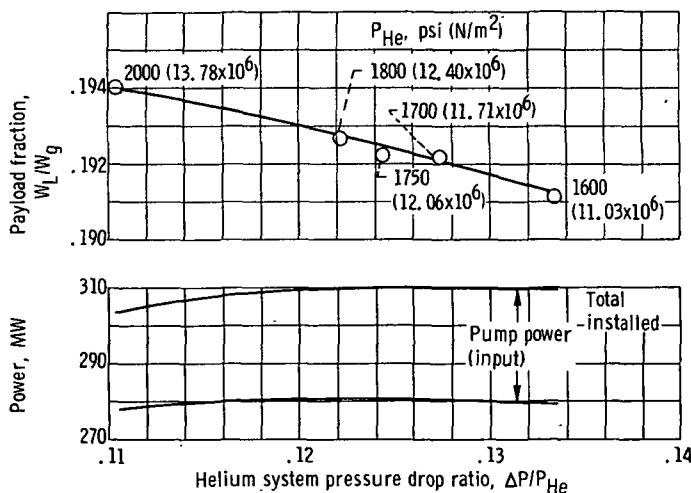

Figure 13. - Effect of helium system pressure. Gross weight, 1x10^6 pounds (453 600 kg); design Mach number, 0.8; altitude, 36 089 feet (11 000 m); shield, metal-water with packing factor of 4/3.

As shown in the figure, the higher helium pressures required slightly less installed power, had less pressure drop ratio, and hence less shaft power extraction from the engines. This allowed a higher efficiency for the engine cycle and hence less chemical fuel was required which accounted for about one-third of the small improvement in payload. The remainder of the improvement was primarily concentrated in the smaller shield, heat exchangers, pumps, and reactor weights associated with the smaller sizes at the higher system pressures. The small increases in duct and engine weights caused by increasing system pressure were easily counter-balanced by the previously mentioned factors.

The variation with Mach number of the total system helium pressure drop ratios and the distribution by components is presented in figure 14 for the nominal helium pressure
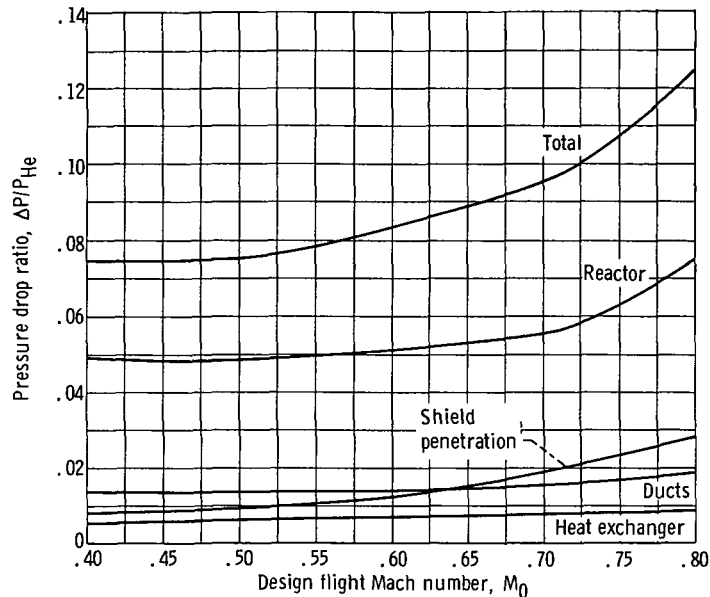
Figure 14. - Variation of component pressure drop ratios with design
flight Mach number. Gross weight, 1×10^6 pounds (453 600 kg);
altitude, 36 089 feet (11 000 m); shield, metal-water with packing
factor of 4/3.

of 1750 psia (12.06 N/m^2). The accompanying variation in pump and installed power is
given in tables II and III. (It should be noted that the component pressure drop ratios
are not additive in the form presented since each is based on the entrance pressure for
that component.) The increase in system pressure drop ratio from 0.075 to 0.124 over
the Mach number range of 0.4 to 0.8 is primarily due to the increases for the reactor
and shield components. This occurs as the installed power increases with Mach number
(see tables II and III). There is a trade-off between the savings in powerplant weight for
smaller reactor radius (shield weight effect) and the increased pumping requirements.
The pressure drop ratios shown represent the best combination that maximizes payload
and not necessarily the minimum pressure drop for any one component. This is also an
example of the reason that performance-weight relations are needed for the major com-
ponents.

Effect of specific engine weight. - The effect of improving the specific engine weight
is shown in figure 15 for the 1-million-pound (45.4$\times 10^4$-kg) airplane. The system per-
formance has been reoptimized. A significant improvement of about 28 000 pounds
(12 690 kg) of payload (2.8 percent of gross weight) was obtained for either the turbofan
or turbojet at Mach 0.6 or 0.8 for a reduction in engine weight of 40 percent (engine
weight is about 6 percent of the gross weight).

Effect of fuselage length and reactor shield fairing. - As discussed in a previous
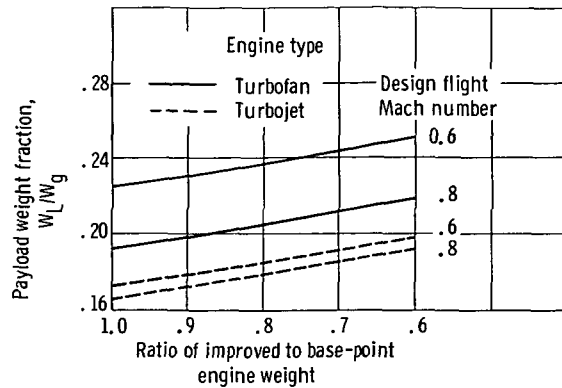section, some of the high altitude and/or Mach number design cases (fig. 5(a)) had such

Figure 15. - Effect of engine technology on performance of the optimized system. Gross weight, 1×10^6 pounds (453 600 kg); altitude, 36 089 feet (11 000 m); shield, metal-water with packing factor of 4/3.

low payload fractions that the fuselage size exceeded the need. Therefore, the effects of placing the reactor within the cargo bay (thus restricting the maximum length of cargo items and drive-through capability) and also of shortening the fuselage were investigated. Results are presented in figure 16.

Over the limited range of conditions investigated, the payload gains realized by reducing the size of the reactor-shield fairing were generally less than 4000 pounds (1814 kg) for the 1-million-pound (45. 4×10^4-kg) airplane. This is a trade-off between a small reduction in installed power due to slightly improved lift-drag ratio (less surface

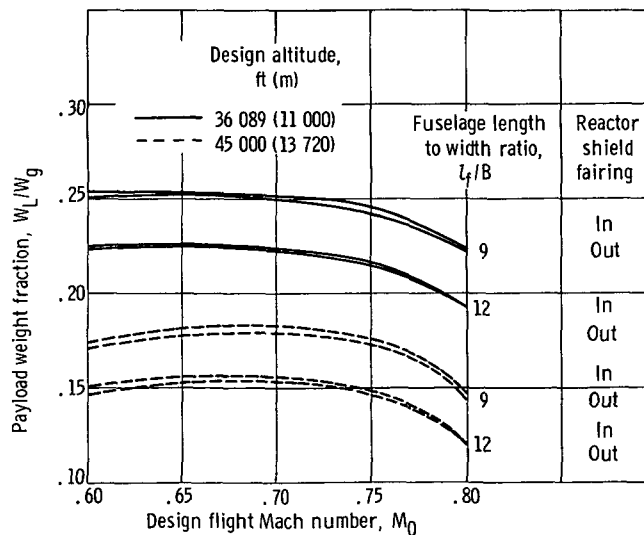Figure 16. - Effect of fuselage size changes on performance of optimized system. Gross weight, 1×10^6 pounds (453 600 kg); shield, metal-water with a packing factor of 4/3.
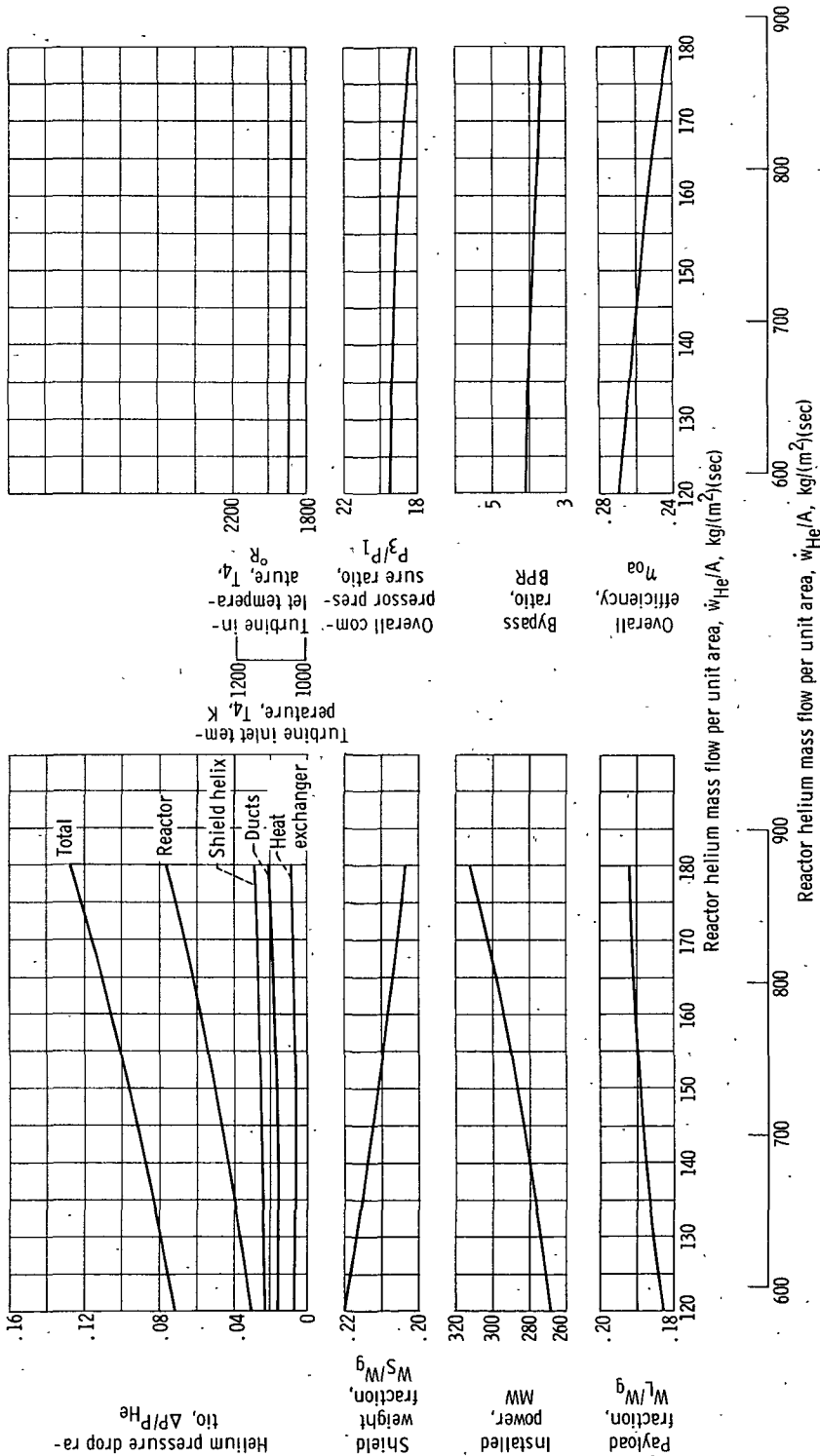
Figure 17. - Effect of reactor helium weight flow per unit area on system performance. Gross weight, 1×10^6 pounds (453 600 kg); altitude, 36 089 feet (11 000 m); shield, metal-water with packing factor of 4/3.

(a) Payload and nuclear side parameters.

(b) Engine cycle parameters.

area) and some increase in fuselage weight as the section moment of inertia is decreased (eq. (E16)).

Decreasing the fuselage length to width ratio from 12 to 9 resulted in a payload increase of between 20 000 and 30 000 pounds (9070 and 13 600 kg). The fuselage profile drag was reduced about 25 percent (or about 7-percent reduction in airplane profile drag) thus increasing the lift-drag ratio about three-tenths of a unit and concommitantly decreasing the installed reactor power. As the fuselage is shortened, the dose distance decreases from 130 to 97. 5 feet (39. 6 to 29. 72 m) and increases the shield weight fraction, according to equation (2), about 10 percent, or 20 000 pounds (9070 kg). This shield weight rise is balanced, in general, against a fuselage weight decline of 40 000 pounds (18 140 kg) to arrive at the cited advantage.

Effect of reactor helium flow rate per unit area. - A typical performance map for a family of reactor designs has been shown in figure 2. The power level and helium weight flow per unit area (of coolant passage) are used to establish both a core radius and a correlation factor used in the shield weight calculations (see eq. (1)). The choice of using a higher reactor flow rate per unit area to obtain a smaller and lighter shield must be balanced against the consequences of an increased pressure drop.

As shown in figure 17(a), payload fraction increased with reactor helium flow rate per unit area only about 5 percent or 1 percent of gross weight over the range considered ($\dot{w}_{He}/A$ of 120 to 180 (586 to 879 kg/(m^2)(sec)); $\Delta P/P_{He}$ reactor 3 to $7\frac{1}{2}$ percent) at Mach 0. 8 and 36 089 feet (11 000 m) in altitude. Notice that the shield weight fraction decreases about 2 percent of gross weight as $\dot{w}_{He}/A$ and installed power increase because of the smaller core size. Installed power increases for the following reason: Increasing the reactor flow rate parameter $\dot{w}_{He}/A$ causes an increase in the core pressure drop (fig. 17(a)), and hence the total pressure drop, which increases the pump power required, and because the pump is shaft powered, engine efficiency decreases (fig. 17(b)). This decrease in engine efficiency increased the chemical fuel allowance about 1 percent of gross weight. Other components of the powerplant group, in addition to the shield and chemical fuel underwent readjustment, with the net result of very little change in this weight fraction. However, the structural weight fraction was reduced slightly more than 1 percent of gross weight primarily due to a lighter wing. Thus, the final result was dependent on interactions among many components, primarily following the network previously established such as in the section Effect of gross weight (p. 26).

Shield technology. - Thus far, all the results presented have been for the metal-water ''base-point'' shield with a packing factor (or shield weight multiple) of 4/3. The difference between the metal-water and hydride-water shields and the meaning of the term packing factor are discussed in the section Shield (p. 12). The variation of payload fraction with packing factor for both shield designs is shown in figure 18. Packing factor and shield technology, both representing substantial adjustments in shield weight, were
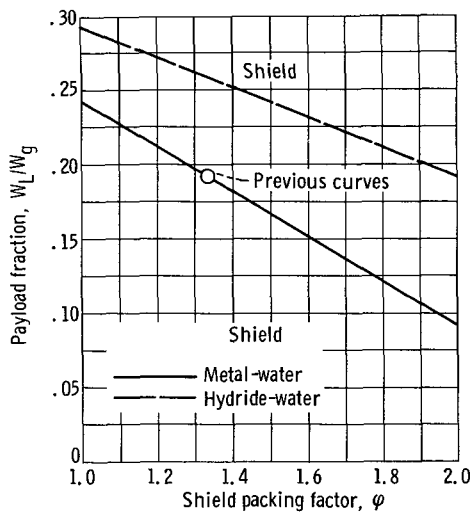
Figure 18. - Variation of payload weight fraction with packing factor and shield technology. Gross weight, 1x10^6 pounds (453 600 kg); design Mach number, 0.8; altitude, 36 089 feet (11 000 m).
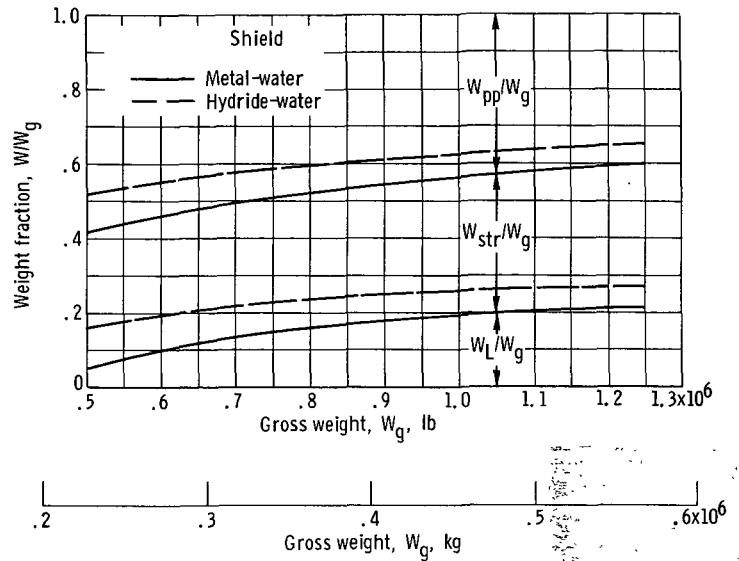

Figure 19. - Influence of shield technology on major weight fraction as function of gross weight. Design Mach number, 0.8; altitude, 36 089 feet (11 000 m); shield packing factor, 4/3.

very important. In fact, the combination of advanced shield materials (hydrides) and a very small packing factor (≈ 1.0) could increase the payload fraction by a factor of 50 percent compared with the previous result for metal-water shields having a packing factor of 4/3. The improvement in payload fraction due to shield technology is shown in figure 19 to be very beneficial over the range of gross weights from 1/2 to $1\frac{1}{4}$ million pounds (226 700 to 566 500 kg) and more important at the lower gross weights where powerplant weight components, the shield in particular, account for the general decrease in payload fraction.

With advanced shield technology, the payload fraction of 16 percent obtained for the 1/2-million-pound (226 700-kg) airplane is about three times that for the metal-water shield with a packing factor of 4/3; however, at $W_g = 10^6$ pounds (453 600 kg) the advantage decreases to 1.3.

Component sensitivity factors. - Two concepts of sensitivity factors are possible depending on whether or not the design is considered frozen. If the system design is frozen and the performance of a certain component must be revised, the design (operating points) of the remaining components is not altered, and the term "fixed" is applied. On the other hand, if the revised performance of a component can be offset by redesigning or reoptimizing the other components, the term "reoptimized" or "rubber" is used.

Examples of each type of sensitivity factor are given in table V for each of the independent variables (listed in Optimization Procedure (p. 19) and appendix F). Where possible, a ±10 percent change was used. The data are for the base-point case of

TABLE V. - SENSITIVITY FACTORS FOR 1-MILLION-

POUND $(45.4 \times 10^4$ kg$)$ AIRPLANE

[Mach number, 0.8; altitude, 36,089 ft (11 000 m); shield, metal-water with packing factor of 4/3.]

Variable	Percent change in variation[a]	Fixed	Rubber
		Percent decrease in payload	
P_3/P_1	10	5.17	0.52
	-10	3.38	.67
P_3/P_2	10	2.2	0.26
	-10	4.4	.39
P_{4a}/P_3	2.85	0.27	0.29
	-2.85	.69	1.02
BPR	10	0.22	0.23
	-10	.314	.306
AR	10	0.32	0.28
	-10	.81	.79
C_L	10	0.8	0.63
	-10	.581	.579
T_4	10	12.54	5.77
	-5	3.8	1.53
ΔP_{HX}	10	0	0
	-10	0	0
ΔP_{ducts}	10	0	0
	-10	0	0
$\dot{w}_{He}/A$	-10	1.12	1.43
$T_{HX, out}$	10	8.0	4.7
	-10	7.6	2.6
T_{He}	-10	11.6	7.3
H	10	13.75	13.9
	-10	[b]3.4	[b]3.88
M_0	10	21.94	18.97
	-10	[b]9.4	[b]15.5

[a]Any change less than tolerance of convergence is considered zero.

[b]Gain.

$M_0 = 0.8$, altitude of 36 089 feet (11 000 m), metal-water shield, packing factor of 4/3, and $W_g = 10^6$ pounds (45.4×10^4 kg). Since the system was optimized, all of the sensitivity factors are negative or zero if the result was less than the computing tolerance.

The independent variables that were most sensitive to change were, in order of relative importance, turbine inlet temperature, helium temperature out of reactor, helium temperature out of heat exchanger, and overall and compressor pressure ratios. Allowing reoptimization decreased the sensitivity factors; for instance, those involving temperature were reduced by about 50 percent. For a few independent variables (negative P_4/P_3 values and $\dot{w}_{He}/A$) a greater sensitivity is indicated for the reoptimized or "rubber" case and was the result of the selected convergence tolerance on payload.

Comparison With Conventional Aircraft

The estimated performance of the nuclear aircraft is compared in figure 20 with the payload-range values predicted for the Air Force C-5A airplane. (The C-5A is the largest logistics aircraft under construction at this time.) Data are presented for both one-way and round trips, no refueling missions. Gross weights of 1.25, 1.0, and 0.73 million pounds (56.7×10^4, 45.4×10^4, and 33.1×10^4 kg) are shown for the nuclear plane, the latter value being approximately equal to that for the C-5A. For round-trip flights, the chemical fuel for an additional takeoff and landing at the midway point has been deducted from the payload for the nuclear planes. The flight Mach number of 0.8 for the nuclear plane is approximately equal to that for the C-5A.

For equal gross weights, the nuclear plane has superior performance for ranges greater than about 5900 nautical miles ($\sim11\times10^6$ m) for one-way missions or about 2700 miles ($\sim5\times10^6$ m) for no-refueling round trips with payload delivery at the midway point. A 1-million-pound (45.4×10^4 kg) nuclear airplane would exceed the payload of the C-5A at ranges beyond 3700 nautical miles (6.9×10^6 m) for one-way trips or beyond about 2000 nautical miles (3.7×10^6 m) for round trips. Payload estimates for the $1\frac{1}{4}$-million-pound (56.7×10^4-kg) nuclear plane exceed those for the C-5A at all ranges of interest for either one-way or round trips. The nuclear airplane's virtually unrestricted range (or, more correctly, endurance) is only limited by human capabilities and equipment reliability.

Flight and ground handling considerations are not comparable for the two systems. However, the use of a unit shield and low dose rates averts some of the operational problems encountered in prior nuclear airplane concepts. No penalties have been assessed for crash safety provisions such as energy absorption systems for the nuclear airplane.

Technology advances in aerodynamics, propulsion, and structures would be mutually
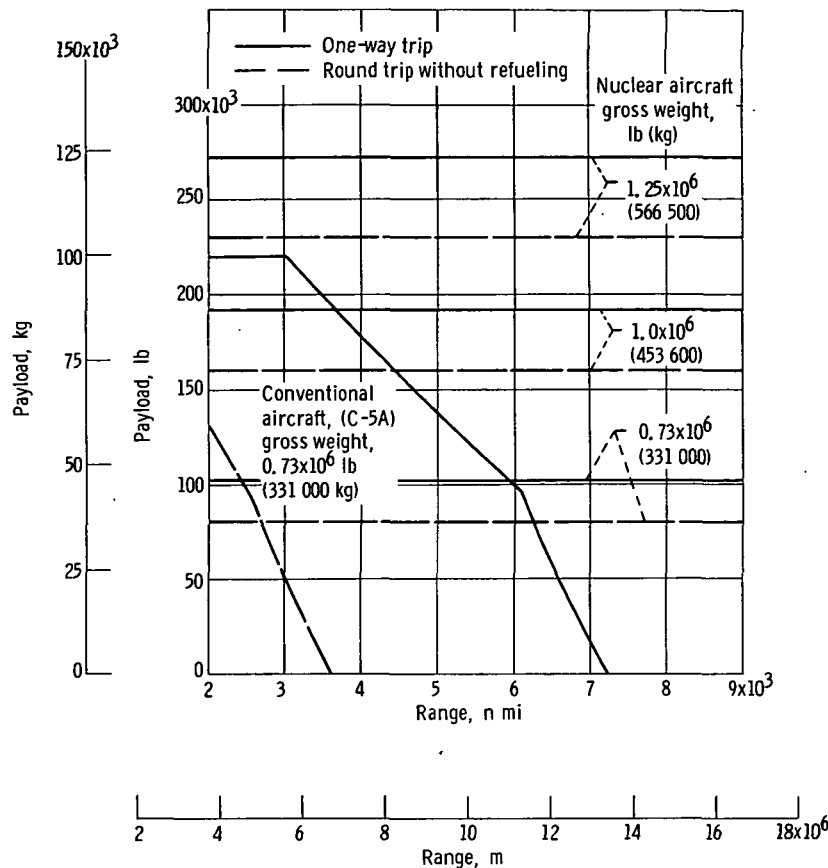
Figure 20. - Comparison of nuclear and conventional fossil fueled aircraft on the basis of payload and range. Nuclear aircraft's design flight Mach number, 0.8; altitude, 36 089 feet (11 000 m); shield, metal-water with a packing factor of 4/3.

beneficial for either the nuclear or conventional planes, whereas advances in nuclear technology would, of course, only benefit the nuclear concept.

SUMMARY OF RESULTS

A preliminary design-point investigation of a subsonic logistic aircraft powered during cruise by a helium-cooled unit-shielded thermal nuclear reactor has been conducted. A range of flight design points, engine cycle parameters for both turbojets and turbofans, reactor coolant flow rates, and pressure have been considered. Variations in gross weight and shield and engine technology were studied, as well as the interrelations and sensitivity factors of the major components. The maximum helium temperature was 2360° R (1311 K) and the nominal maximum reactor wall temperature was 2560° R (1422 K). For the base-point or standard calculation, the helium pressure was

1750 pounds per square inch (12. 06×10^6 N/m^2), and a metal-water shield with a fabricated over ideal weight ratio of 4/3 (called packing factor) was used. The radiation dose level was constant at the very low value of 2. 5 millirem per hour at the flight deck, and for 1000 hours of flight duty corresponds to only one-half the man-year recommendation of the Federal Radiation Council. Payload capacity was selected as the figure of merit to be maximized. The following results were obtained:

1. For the 1-million-pound (45. 4×10^4-kg) gross weight state-of-the-art configuration, the payload fraction was 19 percent for a design altitude of 36 089 feet (11 000 m) at Mach 0. 8. The effect of increasing design altitude and Mach number was to decrease the payload. At lower design altitudes and Mach numbers (20 000 ft (6096 m) and 0. 5) payload fractions increased to about 26 percent; however, such ceiling limited airplanes may be of limited operational value. For the Mach 0. 8, 36 089-foot (11 000-m) design point, the turbofan bypass ratio was 3. 6, the overall pressure ratio was 18. 4, the turbine inlet temperature was 1890° R (1049 K), and the pressure drop between the compressor and turbine due to the heat exchanger was 12 percent. On the nuclear side of the system, the installed power was 309 megawatts (including 9 percent for pump power), the helium pressure was 1750 psi (12. 06×10^6 N/m^2), and the pressure drop was 12 percent. The airplane had an optimum wing loading of 85 pounds per square foot (415 kg/m^2) and a structural weight fraction of 36. 7 percent including equipment and systems.

2. Since shield weight represented about 20 percent of the gross weight for the 1-million-pound (45. 4×10^4-kg) airplane, shield technology had an important effect. At a design Mach number of 0. 8 and an altitude of 36 089 feet (11 000 m), the payload fraction could be increased 30 to 50 percent by using a hydride-water shield material rather than the metal-water type used as the standard case.

3. Payload fraction increased with gross weight at a declining rate up to the largest considered. The value for the 1/2-million-pound (226 700-kg) airplane was 5 percent and increased to 19 and 22 percent, respectively, for 1- and $1\frac{1}{4}$-million-pound (45. 4×10^4- and 56. 7×10^4-kg) airplanes designed for Mach 0. 8 and 36 089 feet (11 000 m). Although the shield was still the predominate weight fraction component and decreased as gross weight increased, the weight fractions of the structure and a group composed of the engines, heat exchangers, and chemical fuel for nonnuclear operation increased.

4. The optimum turbine inlet temperature for maximum payload was within the range of 1800° to 2100° R (1000 to 1249 K), depending on the flight design point. For M_0 = 0. 8 and 36 089 feet (10 990 m), a turbine inlet temperature of 1890° R (1049 K) maximized payload which varied only 7 percent for turbine temperatures between 1800° and 2100° R (1000 to 1249 K) because the other components were allowed to reoptimize. At these higher than optimum turbine temperatures, heat exchanger weight was increasing more rapidly than the engine weight decreased.

5. Varying the system pressure from 1600 to 2000 psia (11.03×10^6 to 13.78×10^6 N/m^2) increased the payload fraction only about 1.5 percent, mainly due to reductions in installed and pump power.

6. The payload fraction obtained with the optimized system using the turbofan cycle was 16 percent greater than for the turbojet cycle at Mach 0.8, and 108 percent greater at Mach 0.4 for a design altitude of 36 089 feet (11 000 m). The overall efficiency for the turbofan cycle was 5 or 8 efficiency counts higher, while the optimum overall compressor pressure ratio was higher for the turbojet. The optimum turbine temperature for the turbofan was generally 100° to 200° F (55.5 to 111 K) higher than for the turbojet.

7. Sensitivity effects due to perturbing the independent variables were more pronounced when considered individually (fixed design) than when other independent variables were allowed to reoptimize. In general, the off-optimum temperature effects were more detrimental.

8. Comparison with the C-5A class of airplanes at equal gross weights ($\sim 7.3 \times 10^5$ lb; 331 000 kg) indicates superior payloads for the nuclear plane for ranges beyond 5900 nautical miles ($\sim 11 \times 10^6$ m) for one-way trips or 2700 nautical miles ($\sim 5 \times 10^6$ m) for round trips without refueling.

Lewis Research Center,
    National Aeronautics and Space Administration,
        Cleveland, Ohio, April 1, 1968,
            789-50-01-01-22.

APPENDIX A

TURBOFAN-JET WEIGHT AND COMPONENT ASSUMPTIONS

The engine weight equation was taken to be of the form

$$W_{eng} = \left(\frac{W_{eng}}{F}\right)_{SLS} F_{SLS}$$

where the specific weight at sea level static $\left(W_{eng}/F\right)_{SLS}$ was assumed to be a function of overall pressure ratio, bypass ratio, and technology level. The sea level static thrust F_{SLS} is computed from the cruise thrust and factors that account for design altitude, Mach number, and turbine inlet temperature. In particular,

$$\left(\frac{W_{eng}}{F}\right)_{SLS} = f_1\left(\frac{P_3}{P_1}\right) f_2\,(BPR)\, f_3(T_4)\, \frac{W_{eng}}{F}$$

where

$$f_1\frac{P_3}{P_1} = \begin{cases} 0.834\,\exp\left(\dfrac{P_3/P_1}{110.0}\right) & \text{(2-spool engines)} \\[4mm] 0.722\,\exp\left(\dfrac{P_3/P_1}{55.5}\right) & \text{(1-spool engines)} \end{cases}$$

$$f_2\,(BPR) = 0.97 - 0.001\,(BPR) + 0.0014\,(BPR)^2$$

$$f_3(T_4) = \left[1 + 5.5{\times}10^{-4}\,(T_4 - 2060)\right]^{-1} \qquad (T_4 \text{ in } {}^{\circ}R)$$

$\dfrac{W_{eng}}{F}$ = reference specific weight (function of technology level), assumed to be 0.213 at $P_3/P_1 = 20$, BPR = 5, and $T_4 = 2060^{\circ}$ R
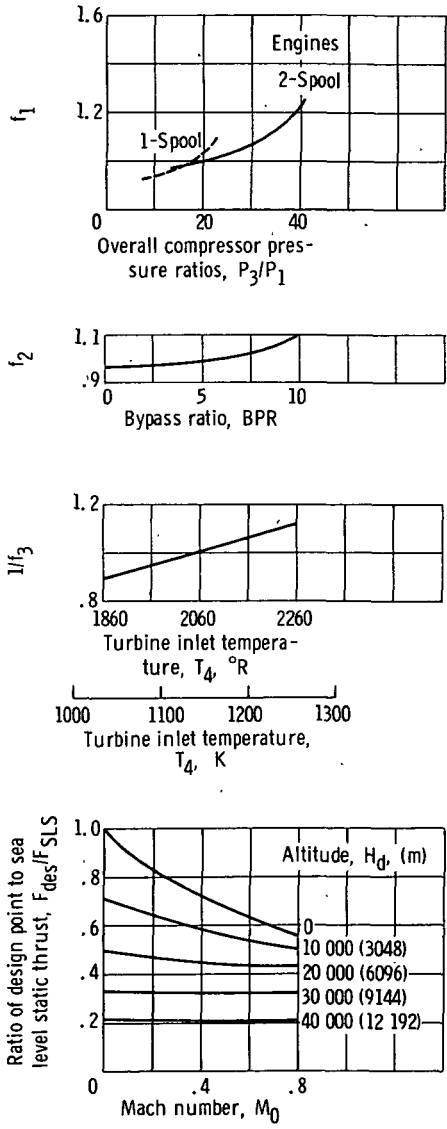
Figure 21. - Values of parameters used in engine weight equation.

$$\frac{F_{SLS}}{F_{des}} = \frac{\sqrt{\psi}}{\alpha}\left[1 + M_0\left(\frac{\psi - \psi^*}{1 - \psi^*}\right)^2\right] \qquad (\psi^* = \psi \text{ at 36 000 ft})$$

The last relation is not valid if BPR > 8 or for altitudes less than 20 000 feet if BPR < 3.

Although F_{SLS}/F_{des} is also a function of BPR, its dependence on BPR is quite small at the high design altitudes (e. g., 36 000 ft) of major interest here. It is also a good approximation at lower design altitudes when BPR ~ 4. These f factors and the F_{SLS}/F_{des} function were selected after compiling data from various engine designs and prototype studies and are displayed in figure 21. Table VI gives the component efficiencies assumed for this study.

TABLE VI. - COMPONENT EFFICIENCIES AND

PRESSURE RATIOS

Component	Assumed efficiency, percent
Fan	0. 88 (adiabatic)
Compressor	. 86 (adiabatic)
Turbine (fan)	. 90 (adiabatic)
Turbine (compressor)	. 90 (adiabatic)
Fan duct thrust coefficient	. 985
Primary nozzle thrust coefficient	. 985
Pressure ratio in primary nozzle	. 98
Inlet pressure recovery	1. 0
Pressure ratio in duct nozzle	. 97
Pressure ratio between turbine inlet and compressor outlet exclusive of heat exchanger	. 95

APPENDIX B

TAYLOR EXPANSION FOR REACTOR PERFORMANCE MAP AND
EQUATIONS FOR SHIELD WEIGHTS AND RADIUS

Taylor expansions were used to curve fit results from the reactor analysis to relate the reactor power, pressure drop, helium temperature, radius, and helium weight flow per unit area. The following terms are used to simplify the expressions developed:

$$\Delta T_{in} = T_{in} - T_{in, o}$$

$$\Delta T_{ex} = T_{ex} - T_{ex, o}$$

$$\Delta P_{in} = P_{in} - P_{in, o}$$

$$\Delta \mathscr{P} = \mathscr{P} - \mathscr{P}_o$$

$$\frac{\Delta W}{A} = \frac{W}{A} - \left(\frac{W}{A}\right)_o$$

where the nominal maximum reactor wall temperature is constant at 2560° R, T_{in} is the helium pump helium exit temperature (^{O}R), T_{ex} the reactor helium exit temperature (^{O}R), P_{in} the reactor inlet helium pressure (psia), $\mathscr{P}$ the reactor power (MW), and W/A the reactor helium flowrate per unit free area (lb/sec/ft^2). The subscript o denotes the reference point values of 1260° R, 2260° R, 1500 psia, 250 megawatts, and 120 pounds per second per square foot, respectively (equivalent to $\dot{w}_{He}/A$ in main body of report).

The expansion for pressure drop can be written in a simplified manner by defining

$$g_1 = \exp\left[9.2696 \times 10^{-3} \left(\frac{W}{A}\right)_o\right]$$

$$g_2 = \exp\left(-2.215 \times 10^{-3} P_{in, o}\right)$$

Then,

$$\Delta P_{rea} = \Big[0.0145\, g_1 - 0.02 - 1.027 \times 10^{-5}\, \Delta T_{in} + (2.24 \times 10^{-7}\, T_{ex,\,o} - 4.427 \times 10^{-4}) \Delta T_{ex}$$

$$+ 1.12 \times 10^{-7} (\Delta T_{ex})^2 + 1.345 \times 10^{-4}\, g_1 \frac{\Delta W}{A}$$

$$+ 6.25 \times 10^{-7}\, g_1 \left(\frac{\Delta W}{A}\right)^2 - 1.0034 \times 10^{-3}\, g_2\, \Delta P_{in}$$

$$+ 1.111 \times 10^{-6}\, g_2 (\Delta P_{in})^2 - 8.2033 \times 10^{-10}\, g_2 (\Delta P_{in})^3 \Big]\, 1.3889$$

The reactor radius was calculated from the Taylor expansion:

$$R_{rea} = 1.42206 \times 10^{-5} \left(\frac{W}{A}\right)_o^2 - 6.9255 \times 10^{-3} \left(\frac{W}{A}\right)_o + 2.5973 + 3.1593 \times 10^{-3}\, \Delta \mathscr{P}$$

$$+ \left[2.84412 \times 10^{-5} \left(\frac{W}{A}\right)_o - 6.9255 \times 10^{-3} \right] \frac{\Delta W}{A} + 1.42206 \times 10^{-5} \left(\frac{\Delta W}{A}\right)^2$$

The T_{in} and T_{ex} terms do not appear in this expression because their effect on R was negligible as determined from detailed calculations over the range of temperatures used herein.

Reactor weight was calculated from

$$W_{rea} = 24.72\, \mathscr{P} + 682$$

which was then doubled to account for moderator (water) to air heat exchanger and after-heat removal system weights.

A curve fit to f, which is in reality a measure of the reactor core density, was then found:

$$R_{rea}\ (\text{in cm}) = 30.48\ R\ (\text{in ft})$$

$$R_1 = -10^{-5} \mathscr{P}^2 + 0.089\, \mathscr{P} + 44.9750$$

$$R_2 = -3.5 \times 10^{-5} \mathscr{P}^2 + 0.097\, \mathscr{P} + 48.6375$$

$$R_3 = -4.5 \times 10^{-5} \wp^2 + 106 \wp + 51.5125$$

$$C_1 = R_2^2 - R_{rea}^2 \text{ (in cm)}$$

$$C_2 = R_2 - R_1$$

$$C_3 = R_3^2 - R_2^2$$

$$C_4 = R_3 - R_2$$

$$X = \frac{C_3 - C_1}{C_3 C_2 - C_1 C_4}$$

$$Y = \frac{1 - C_2 B}{C_1}$$

$$Z = 1 - YR_1^2 - XR_1$$

Then,

$$f = YR_{rea}^2 \text{ (in cm)} + XR_{rea} \text{ (in cm)} + Z$$

If $f < -4$, set $f = -4$.

For base-point shields (metal-water),

$$R_s = (113.5 + 2.5 f) \frac{\wp^{0.122}}{30.48}$$

$$W_s = (17\,900 + 1100f) \wp^{0.407}$$

For advanced shields (hydride-water),

$$R_s = (85 + 2.0 f) \frac{\wp^{0.134}}{30.48}$$

$$W_s = (12\,100 + 1000f) \wp^{0.419}$$

APPENDIX C

CHEMICAL FUEL ALLOWANCE

The amount of fuel required for the chemical flight phases is primarily dependent on the engine specific fuel consumption (sfc), the basic design altitude and Mach number, and the emergency range (or duration). To compute the fuel allowance, the total fuel requirement was broken down into three parts: ascent, cruise, and descent. Thus,

$$W_F = W_{F, TC} + W_{F, c} + W_{F, d} \tag{C1}$$

Ascent Fuel $W_{F, TC}$

The climb fuel requirement can be approximated by energy balance relations. The change in energy per pound of aircraft weight (specific energy) may be written (ref. 10, eq. 2)

$$W \, de = \eta_{oa} HV \, dW_{F, TC} - DV_0 \, dt \tag{C2}$$

where W is the aircraft weight, e its specific energy, η_{oa} the engine overall efficiency, HV the fuel heating value, D the airplane drag, V_0 the flight velocity, and t the time. Since $dH = V_0 \sin \sigma \, dt$, where σ is the path angle, equation (C2) may be rearranged and formally integrated to give

$$\int_0^{W_{F, TC}} \eta_{oa} HV \, dW_{F, TC} = \int_{e_1}^{e_2} W \, de + \int_0^{H_d} \frac{D}{\sin \sigma} \, dH \tag{C3}$$

This equation is still exact; that is, it accounts for the energy change due to change in gross weight as fuel is burned. Defining $\overline{\eta}_{oa}$ to be the average efficiency and $\overline{W}$ to be the average weight during climb, equation (C3) can be solved for the climb fuel:

$$W_{F, TC} = \frac{\overline{W} \, \Delta e + \int_0^{H_d} \frac{D}{\sin \sigma} \, dH}{HV \overline{\eta}_{oa}} \tag{C4}$$

For a first-order approximation, $\overline{W}$ can be taken to be the same as the takeoff weight. Also, η_{oa} can be considered to be independent of altitude but varying from zero at $V = 0$ to cruise efficiency $\eta_{oa, c}$ at $V = V_0$. Thus, for a change in altitude only, $\overline{\eta}_{oa}$ would be taken to be $\eta_{oa, c}$. But for an increase in velocity from zero to V_0, $\overline{\eta_{oa}}$ would be taken to be $1/2 \, \eta_{oa, c}$. And if during climb both velocity and altitude change, then $\overline{\eta}_{oa}$ could be calculated as the sum of two weighted terms - one term associated with the change in kinetic energy KE and the other potential energy PE. For simplicity, the function chosen was

$$\overline{\eta}_{oa} = \left(\frac{1}{2} \frac{\Delta KE}{\Delta E} + 1.0 \frac{\Delta PE}{\Delta E} \right) \eta_{oa, c} \tag{C5}$$

where ΔE is the change in total aircraft energy during climb (i.e., $\Delta E = \overline{W} \Delta e$).

The integral of $D/\sin \sigma$ was approximated by rewriting it as:

$$\int_0^{H_d} \frac{D}{\sin \sigma} \, dH = \int_0^{H_d} \frac{C_D \frac{1}{2} \rho V_0^2 S_w}{\sin \sigma} \, dH = \frac{\overline{C_D} S_w}{2 \sin \overline{\sigma}} \int_0^{H_d} \rho V_0^2 \, dH \tag{C6}$$

where again bars denote flight path averages. The integral of ρV_0^2 can be approximated by assuming that the climb path is a straight line on a M-H diagram between the points $(0.25, 0)$ and (M_d, H_d). Then,

$$M = aH + b$$

where

$$a = \frac{M_d - 0.25}{H_d}$$

$$b = 0.25$$

Also

$$V_0^2 = M^2 \gamma RT \qquad (\gamma = 1.4)$$

$$T = \begin{cases} T_{SL} - 0.003566\ H & (0 \leq H \leq 36\ 089\ \text{ft}) \\ 390^\circ\ R & (H > 36\ 089\ \text{ft}) \end{cases}$$

$$\rho = \begin{cases} \rho_{SL}\left(\dfrac{T}{T_{SL}}\right)^{4.256} & (0 \leq H \leq 36\ 089\ \text{ft}) \\ \rho_{36\ 089}\ \exp\left(-\dfrac{H - 36\ 089}{2.08\times10^4}\right) & (H > 36\ 089\ \text{ft}) \end{cases}$$

Substitution of these relations into equation (C6) and integration give

$$\int_0^{H_d} \rho V^2\,dH = \gamma P_o \left[\frac{b^2 - M_*^2\left(\dfrac{T_d}{T_{SL}}\right)^{6.256}}{4.3\times10^{-5}} + a\,\frac{b - M_*\left(\dfrac{T_d}{T_{SL}}\right)^{7.256}}{1.073\times10^{-9}} + a^2\,\frac{1 - \left(\dfrac{T_d}{T_{SL}}\right)^{8.256}}{6.089\times10^{-14}} \right]$$

$$-\ \gamma P_{36\ 089}\left[\frac{\rho_d}{\rho_{36\ 089}}\left(2.08\times10^4\ M_d^2 + 8.65\times10^8\ aM_d + 18\times10^{12}\ a^2\right)\right.$$

$$\left. -\left(2.08\times10^4\ M_*^2 + 8.65\times10^8\ aM_* + 18\times10^{12}\ a^2\right)\right] \qquad (C7)$$

where

$$M_* = \begin{cases} M_d & (H_d \leq 36\ 089) \\ M_{36\ 089} & (H_d > 36\ 089) \end{cases}$$

The second term of equation (C7) is not required for $H > 36\ 089$. All that remains is to evaluate $\overline{C_D}/\sin\bar{\sigma}$. Letting $C_{D,d}$ be the cruise design value of C_D gives

$$\frac{\overline{C}_D}{\sin \sigma} = \frac{C_{D,d} \dfrac{\overline{C}_D}{C_{D,d}}}{\sin \overline{\sigma}} \approx 28.65\, C_{D,d} \qquad \text{(C8)}$$

where the constant 28.65 was chosen to bring the approximate solution into agreement with several numerically integrated flight path solutions. Substitution of equations (C5), (C6), and (C7) into equation (C4) yields the final equation for $W_{F,TC}$.

The compressor and bypass ratios, P_3/P_1 and BPR, optimized for nuclear cruise were assumed constant during takeoff, climb, and acceleration, while a turbine temperature of 2160° R was selected.

Descent Fuel $W_{F,d}$

The descent fuel is based on a typical value of 2000 pounds per hour at descent conditions for a 300 pound per second airflow turbojet. Thus, for the more general case of a turbofan engine,

$$W_{F,d} = \frac{2000}{300} \frac{\dot{w}_{a,T}}{1 + BPR} \frac{t_d}{3600} \qquad \text{(C9)}$$

The descent time t_d can be approximated by assuming that during descent the L/D ratio remains constant. The range covered during an idle power descent is then $H_d(L/D)$. If the velocity decreases linearly from V_0 to the approach velocity V_{app},

$$V = V_0 - (V_0 - V_{app})\left(\frac{t}{t_d}\right) \qquad \text{(C10)}$$

For large L/D, the range during descent is

$$H_d\left(\frac{L}{D}\right) \cong \int_0^{t_d} \left[V_0 - (V_0 - V_{app})\left(\frac{t}{t_d}\right)\right] dt$$

$$= \frac{1}{2} t_d (V_0 + V_{app}) \qquad \text{(C11)}$$

Thus,

$$t_d = \frac{2H_d\left(\frac{L}{D}\right)}{V_0 + V_{app}} \qquad \text{(C12)}$$

Combining equations (C9) and (C12) yields

$$W_{F,d} = 0.0037 \frac{\dot{w}_{a,T}}{1 + BPR} \frac{H_d\left(\frac{L}{D}\right)}{V_0 + V_{app}} \qquad \text{(C13)}$$

Emergency Cruise Fuel $W_{F,c}$

To achieve a given range R at the design flight conditions, the required fuel is

$$W_{F,c} = D(sfc)t \qquad \text{(C14)}$$

where the drag D is $(W_g - W_{F,TC})/(L/D)$ and the time t is determined by

$$t = \frac{R - H_d\left(\frac{L}{D}\right)}{V_0} \qquad \text{(C15)}$$

Hence,

$$W_{F,c} = \frac{W_g - W_{F,TC}}{\left(\frac{L}{D}\right)} (sfc) \frac{R - H_d\left(\frac{L}{D}\right)}{V_0} \qquad \text{(C16)}$$

The sfc is calculated for the nuclear cruise cycle parameters P_3/P_1, BPR, and T_4.

APPENDIX D

AERODYNAMICS

The variation of maximum fuselage width with gross weight was selected as

$$B = 16.4 + 11.2\left(\frac{W_g}{10^6} - 0.5\right) \tag{D1}$$

The surface area of the fuselage group composed of the basic body, the reactor shield fairing, the gear sponsons, and the dorsal fin was given by

$$S_f = \pi B^2\left(\frac{l_f}{B} - 1\right) + \frac{5\pi}{4}\sqrt{1.56\ R_{sh}^2 + \left[\frac{B}{2}\left(\frac{l_f}{B} - 4.5\right)\right]^2} + \frac{B^2}{2}\left(\frac{l_f}{B} - 6\right) + 750\frac{W_g}{10^6} \tag{D2}$$

Examples of the variation with gross weight of fuselage width, length, surface area, and cargo bay length are given in table VII. The values for fuselage length to width ratios of 12 and 9 are shown as well as having the reactor assembly either within or external to the cargo bay.

TABLE VII. – EXAMPLES OF FUSELAGE DIMENSION PARAMETERS

W_g, lb	B, ft	Reactors exterior to cargo bay (R_{sh} = 7)			Reactors interior to cargo bay (R_{sh} = 0)	
		S_f, ft^2 (l_f/B = 12)	l_f, ft (l_f/B = 12)	l_c, ft (l_f/B = 12)	S_f, ft^2 (l_f/B = 12)	S_f, ft^2 (l_f/B = 9)
0.5×10^6	16.4	11 500	196.7	123	------	------
1.0	22.0	21 100	264.0	165	15 027	13 640
1.25	24.8	26 750	297.5	186	------	------
1.5	27.6	32 500	331.0	207	------	------

The wing thickness ratio perpendicular to the quarter chord line was reduced from the value of 0.18 for Mach numbers greater than 0.65 according to the relation

$$\tau_{w,\perp,1/4} = \frac{0.117}{M_0 + \frac{4}{3}(M_0 - 0.65)} \tag{D3}$$

The thickness ratio of the tail was maintained at 0.12.

The planform taper ratio of the wing was maintained at 0.3 and the sweepback angle was calculated by equation (D4) which has been slightly modified from that given in reference 11:

$$\Lambda_{1/4} = \cos^{-1}\left(\frac{\frac{0.655 - 1.77\,\tau_{w,\perp,1/4}}{1.794C_L} + 0.72}{M_0} - 0.388\right) \tag{D4}$$

Table VIII gives examples of values of wing thickness ratio and sweepback angle with Mach number for a lift coefficient C_L of 0.6.

TABLE VIII. - EXAMPLES OF WING PARAMETERS FOR LIFT

COEFFICIENT OF 0.6

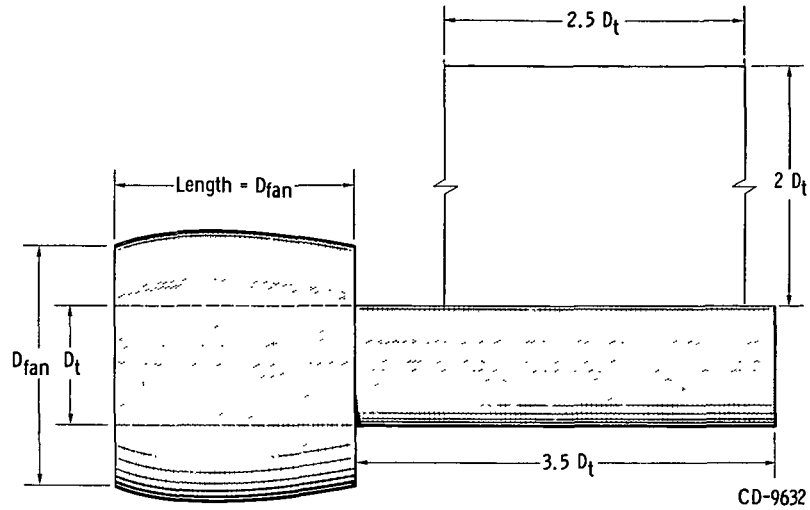| Flight Mach number, M_0	Wing thickness to chord ratio perpendicular to wing quarter chord line, $\tau_{w,\perp,1/4}$	Wing sweepback angle (quarter chord), $\Lambda_{1/4}$, deg	Sweepback correction to induced drag, Q_Λ
0.4 to 0.65	0.18	0	1.0
0.70	.151	0	1.0
.75	.132	22	1.06
.80	.117	30	1.10

Figure 22. - Parametric representation of engine nacelle and pylon strut.

The surface area of the nacelle and pylon depicted parametrically in figure 22 was

$$S_N = \frac{ND_{fan}^2}{BPR + 1}\left(BPR + 4.5 + \frac{10}{\pi}\right) \tag{D5}$$

$$BPR = \left(\frac{D_{fan}}{D_{tip}}\right)^2 - 1 \tag{D6}$$

$$D_{fan}^2 = \frac{4}{\pi N} \frac{F_{inst}}{\dfrac{F}{\dot{w}_a} \, 49.4 \, \dfrac{A^*}{A} \, \dfrac{\delta_0}{\sqrt{\theta_0}}} \tag{D7}$$

with F_{inst} taken from equation (7). The friction drag of the nacelle and pylon was doubled to account for scrubbing and interference effects.

The coefficient of drag due to lift was compiled as

$$C_{D,i} = K_{C,L,\alpha} C_L^2 \tag{D8}$$

$$K_{C,L,\alpha} = \frac{Q_\Lambda}{\pi}\left(\frac{1}{AR} + Q_\lambda\right) + Q_p \tag{D9}$$

where

$$Q_\Lambda = f(\Lambda) \qquad \text{(See table VIII)}$$

$$Q_\lambda = f(\lambda) = 0.0021 \text{ for } \lambda = 0.3$$

$$Q_p = 0.006$$

The general equation used for the profile drag of major components was

$$C_{D,o,i} = A_i \left(\frac{C_{fr} \ell^{1/7}}{\ell_i^{1/7}} + C_{r,o} \right) C_i \tag{D10}$$

The coefficient of friction C_{fr} was calculated using the method of reference 8 for compressible turbulent boundary layer as a function of Reynolds number based on the characteristic length of each major component. The coefficient C_i is used to adjust the friction and roughness drag for other effects such as thickness ratio for the airfoil surfaces (ref. 9):

$$C_i = 1 + 2\tau + 60\tau^4 \tag{D11}$$

APPENDIX E

STRUCTURAL WEIGHT ESTIMATION

The gross weight at the beginning of cruise is used as the basis for structural weight calculations. This differs from the takeoff gross weight by the fuel consumed during takeoff, climb, and acceleration:

$$W'_g = W_g - W_{F, TC} \tag{E1}$$

The flight gross weight can also be expressed in terms used in calculating the weight of the structure as

$$W'_g = W_{f, l} + W_{w, a} + W_w \tag{E2}$$

The term $W_{f, l}$ conceptually includes everything attached to the fuselage other than the wing and can be further defined in terms of structural items, powerplant components, and payload as

$$W_{f, l} = W_{f, a} + W_{fuse} + W_t + W_{fix} + W_{gear} \tag{E3}$$

The total load available in the fuselage for the arrangement herein is the sum of the re-actor and shield (including penetration penalty), $W_{s+p+rea}$, and the payload, W_L:

$$W_{f, a} = W_{s+p+rea} + W_L \tag{E4}$$

The two terms remaining from equation (E2), $W_{w, a}$ and W_w, represent the sum of the weight factors causing bending moment relief in the wing. Items other than the wing weight W_w are included in $W_{w, a}$ which is defined, for the arrangement herein, as

$$W_{w, a} = W_{eng} + W_N + W_{F+tanks} + W_{HXL} \tag{E5}$$

The procedures used for calculating the weights needed to evaluate equations (E2) to (E5) are now given or explained. The weights $W_{s+p+rea}$, W_{HXL}, and W_{eng} are known from separate routines such as appendixes A and B. The weight of the nacelles was es-timated using the engine-pod (nacelle-pylon) surface area from the configuration given in appendix D, and a weight of 3 pounds per square foot:

$$W_N = 3NS_N \tag{E6}$$

The remaining item from equation (E5) that relieves wing bending moment is the chemical fuel and its containment weight referred to herein as chemical fuel plus tanks:

$$W_{F+tanks} = 1.032\,W_F - W_{F,\,TC} \tag{E7}$$

The structural weight of the wing W_w was calculated for $\lambda = 0.3$ using methods similar to those of reference 12:

$$W_w = \cfrac{1}{\cfrac{1 + n_f b_s}{10^6}\left(13.2 + 2.33\,\dfrac{b_s}{t_r}\right)}\left\{2.86\,S_w + 0.00388\,\dfrac{S_w^2}{b_s} + \dfrac{n_f b_s}{10^6}\left[W_g'\left(15.6 + 3.17\,\dfrac{b_s}{t_r}\right)\right.\right.$$

$$\left.\left. - W_{F+tanks}\left(12.8 + 2.06\,\dfrac{b_s}{t_r}\right) - (W_{eng} + W_{HXL} + W_N)\left(14.9 + \dfrac{b_s}{t_r}\right)\right]\right\} \tag{E8}$$

where the structural span is

$$b_s = \frac{b}{\cos \Lambda_{0.4}} \tag{E9}$$

the maximum wing root thickness is

$$t_r = c_r \tau_{w,\perp,\,1/4}\,\cos \Lambda_{1/4} \tag{E10}$$

and the root chord is

$$c_r = \frac{2b}{AR\,(1 + \lambda)} \tag{E11}$$

The structural or equipment weight items in equation (E3) were calculated as follows:

$$W_{fix} = 10\,000 + 0.03\,W_g \tag{E12}$$

$$W_{gear} = W_g \left[0.0515 \left(\frac{W'_g}{10^6} \right)^{0.465} \right] \qquad (E13)$$

$$W_t = 0.012 \left(\frac{S_{ht}}{S_w} + \frac{S_{vt}}{S_w} \right) n_f W_g \qquad (E14)$$

The payload weight is given by

$$W_L = W_{cargo} + W_{crew} + W_{prov} \qquad (E15)$$

The fuselage structural weight was calculated using a slightly modified relation from reference 12:

$$W_{fuse} = C_3 \left(1.3 + \frac{B}{d_f} \right) \left(\frac{\ell_f}{d_f} \right) d_f^2 + C_4 n_f d_f \left(\frac{\ell_f}{d_f} \right)^2 \left(1.3 + \frac{B}{d_f} \right)$$

$$\times \left(2.3 - \frac{B}{d_f} \right) \left(\frac{2}{3} K_f^2 + 2 \frac{1 - K_f}{\ell_f} X_{1/4} \right) W_{f, \ell}$$

$$+ 5B^2 \left(\frac{\ell_f}{B} - 4 \frac{1}{2} B \right) + 16.9 B^2 + 10 \left[\pi(B + d_f) + 8.2 B \right] \qquad (E16)$$

The last three terms in equation (E16) are simple-minded adjustments for cargo floor, pressure bulkheads, and front and rear loading door cutouts.

The maximum depth or height of the fuselage was chosen as

$$d_f = 1.273 B + 1.25 R_s \qquad (E17)$$

$$K_f = K_{c.g.} - \frac{X_{1/4}}{\ell_f} \qquad (E18)$$

$$K_{c.g.} = 0.55$$

$$C_3 = 3.2$$

$$C_4 = \frac{13.24}{10^6}$$

The airframe or structural weight estimated by this procedure corresponds to the usual empty weight minus the dry weight of the engines and is defined by

$$W_{str} = W_w + W_{fuse} + W_t + W_{fix} + W_{gear} + W_{tanks} \tag{E19}$$

APPENDIX F

OPTIMIZATION PROCEDURE

The optimization routine keeps track of the independent variables and the figure of merit. It perturbs the initially guessed independent variables individually, and stores a new value (or guess for the optimum value) for the independent variable if the figure of merit has been improved. After a pass through the entire array of independent variables, perturbation factors are changed and the process is repeated. When the change in the figure of merit at the end of the pass is less than some specified tolerance, the case is terminated and the results outputed (flow chart A, fig. 23). Of course, this procedure does not guarantee an absolute maximum. It may be local, depending on the choice of starting conditions, and several sets of starting conditions may be necessary to determine the absolute maximum. Also, it is possible to obtain nearly the same optimum with different combinations of independent variables. This occurs since a narrow band of alternate selection exists within which the independent variables may be mutually traded without altering the figure of merit (within the convergence tolerance).

The independent variables considered in this study are P_3/P_1, P_2/P_1, P_4/P_3, BPR, T_4, T_{ex}, T_{HX}, W/A, P_{HX}, P_{duct}, AR, and C_L. This choice is arbitrary as long as the independent variables plus fixed inputs are sufficient to completely specify the system. The choice of engine parameters is fairly typical and will determine engine performance if the shaft power extracted for pumping helium is known. In addition, the independent variables specify inlet and outlet air side conditions for the heat exchangers.

Guessed values for the optimum independent variables including AR and C_L with fixed choices of fuselage sizing parameters (appendix D) and an assumed value of C_D yield an initial guess as to the drag of the aircraft. From this, the reactor power is calculated. Then, the reactor power together with T_{ex}, T_{HX}, W/A, and P_{He} size the reactor and shield. These, in turn, adjust the fuselage and engine sizes and determine C_D. This C_D thus becomes a variable in a loop until the new assumed C_D agrees with the calculated one.

Helium side temperatures and pressure drops plus air side conditions from the engine calculations are then used to size the heat exchangers and ducts.

Finally, the numerical value of the power is needed to calculate the helium pressure drop through the reactor - hence, the shaft power to run the pump. Since the power is a function of the pressure drop and visa versa, another loop exists and must be iterated.

The need for an overall optimization procedure becomes apparent when the engine air side, nuclear helium side, and airframe components are optimized independently. For example, if the engine parameters are optimized on the basis of thermal efficiency,

T_4 would increase beyond that obtainable from the heated helium. The limiting factor would have been the growth of heat exchanger weight and of the power required. If L/D is used to design the airframe, the structure weight is so high that the corresponding decrease in engine size and reactor power still results in a net decrease in the value of the figure of merit. If helium side pressure drops are minimized in order to reduce power, the heat exchanger and helium duct weights increase. These are just a few of the trade-offs involved. Engine parameters not only affect engine size, but also the power required - consequently, the helium side conditions. These, in turn, affect reactor size
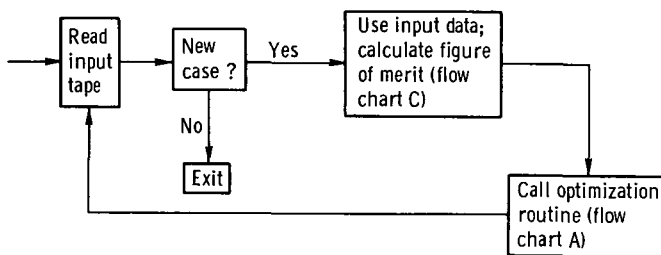

(a) MAIN routine.
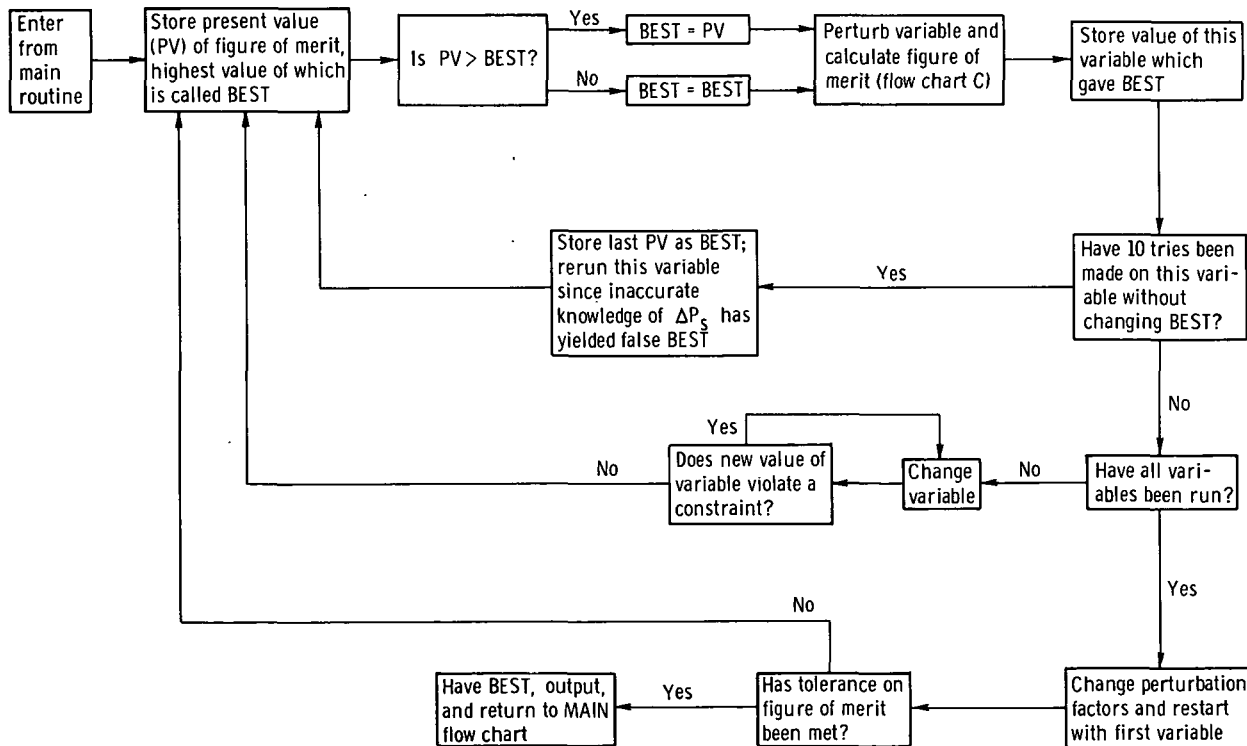

(b) Flow chart A: optimization routine.

Figure 23. - Flow diagrams for airplane-powerplant optimizing procedure.

and thus the fuselage dimensions, which affect the drag and hence the engine size, ad infinitum.

Any other independent variable enters this same loop at some point and the need for a master program to oversee these effects becomes apparent. The overall process can be seen by examining the main, optimization, airplane design, and calculation of figure of merit flow charts (see fig. 23).
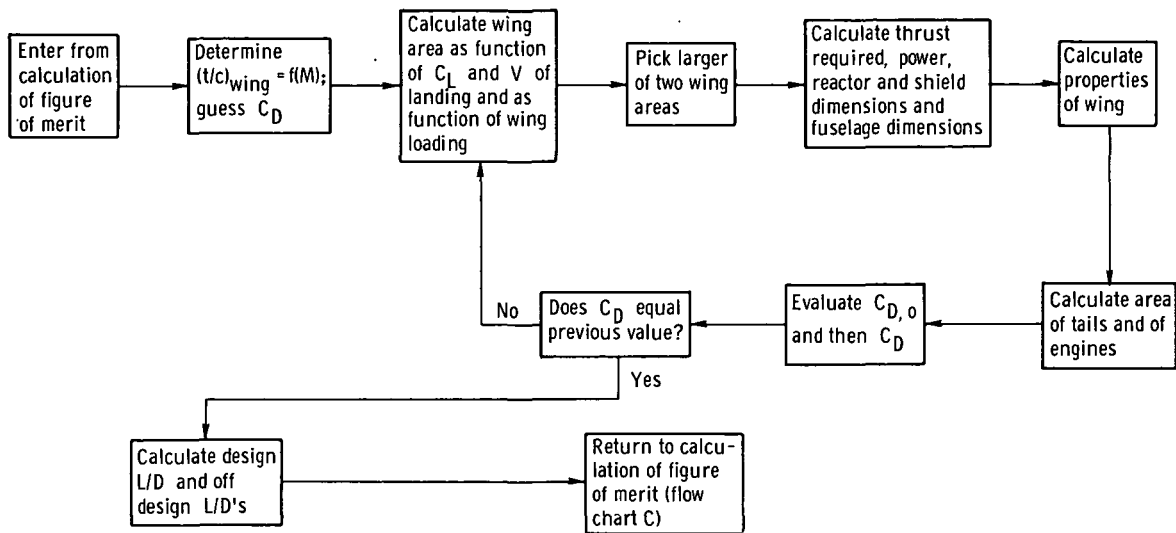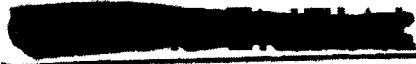

(c) Flow chart B: design of airplane.
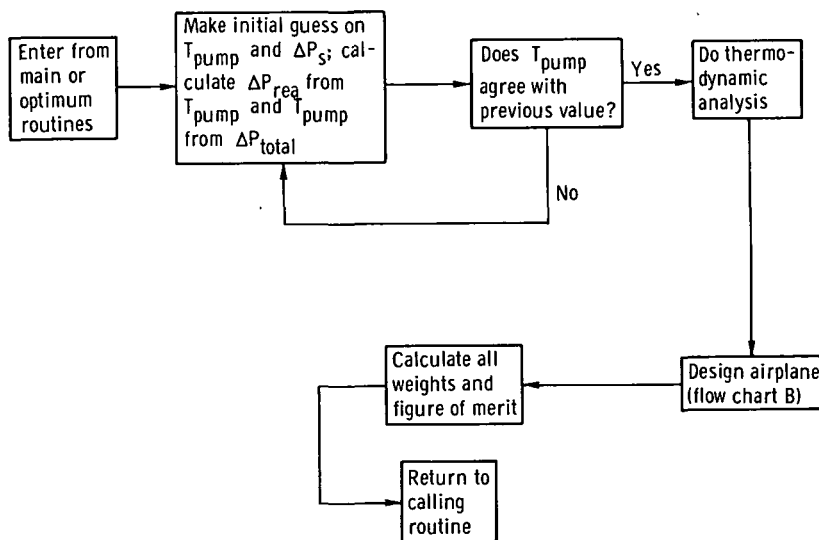
(d) Flow chart C: calculation of figure of merit.

Figure 23. - Concluded.

REFERENCES

1. Anon: Review of Manned Aircraft Nuclear Propulsion Program. AEC and DOD Report to Congress by the Comptroller General of the United States, B-146759, Feb. 1963.

2. Johnson, Paul G.; and Smith, Roger L.: Comparison of Three Nuclear Propulsion Systems for Logistic-Type Aircraft. NASA Memo 3-16-59E, 1959.

3. Cavicchi, R. H.; Ellerbrock, H. H.; Hall, E. W.; Heppler, H. J.; Livingood, J. N. B.; and Schwenk, F. C.: Design Analysis of a Subsonic Nuclear-Powered Logistic Airplane with Helium-Cooled Reactor. NASA TM-X-28, 1959.

4. Pinkel, B.: The Impact of the High Development Cost of Advanced Flight Propulsion Systems on Development Policy. Rep. No. RM-4560-PR, RAND Corp., Oct. 1965. (Available from DDC as AD-624856.)

5. Rom, Frank E.: Subsonic Nuclear Aircraft Study. NASA TM X-1626, 1968.

6. Mittelman, Phillip S.: Advances in Power-Reactor Shield Analysis. Power Reactor Tech., vol. 9, no. 1. Winter 1965-66, pp. 19-24.

7. Kays, W. M.; and London, A. L.: Compact Heat Exchangers. Second ed., McGraw-Hill Book Co., Inc., 1964, p. 186, fig. 10-9.

8. Tucker, Maurice: Approximate Calculation of Turbulent Boundary-Layer Development in Compressible Flow. NACA TN 2337, 1951.

9. Blakeslee, D. J.; Johnson, R. P.; and Skavdahl, H.: A General Representation of the Subsonic Lift-Drag Relation for an Arbitrary Airplane Configuration. Rep. No. RM-1593, RAND Corp., Jan 1, 1955.

10. Rutowski, Edward S.: Energy Approach to the General Aircraft Performance Problem. J. Aeron. Sci., vol. 21, no. 3, Mar. 1954, pp. 187-195.

11. Murrow, R. B.; Schairer, R. S.; and Sturdevant, C. V.: Bomber Capabilities - 1954 Turboprop and Turbojet Powerplants. Rep. No. R-171, RAND Corp., Feb. 1, 1950.

12. Shanley, Francis R.: Weight-Strength Analysis of Aircraft Structures. Second ed., Dover Publ., Inc., 1960.

"The aeronautical and space activities of the United States shall be conducted so as to contribute . . . to the expansion of human knowledge of phenomena in the atmosphere and space. The Administration shall provide for the widest practicable and appropriate dissemination of information concerning its activities and the results thereof."

—NATIONAL AERONAUTICS AND SPACE ACT OF 1958

NASA SCIENTIFIC AND TECHNICAL PUBLICATIONS

TECHNICAL REPORTS: Scientific and technical information considered important, complete, and a lasting contribution to existing knowledge.

TECHNICAL NOTES: Information less broad in scope but nevertheless of importance as a contribution to existing knowledge.

TECHNICAL MEMORANDUMS: Information receiving limited distribution because of preliminary data, security classification, or other reasons.

CONTRACTOR REPORTS: Scientific and technical information generated under a NASA contract or grant and considered an important contribution to existing knowledge.

TECHNICAL TRANSLATIONS: Information published in a foreign language considered to merit NASA distribution in English.

SPECIAL PUBLICATIONS: Information derived from or of value to NASA activities. Publications include conference proceedings, monographs, data compilations, handbooks, sourcebooks, and special bibliographies.

TECHNOLOGY UTILIZATION PUBLICATIONS: Information on technology used by NASA that may be of particular interest in commercial and other non-aerospace applications. Publications include Tech Briefs, Technology Utilization Reports and Notes, and Technology Surveys.

Details on the availability of these publications may be obtained from:

SCIENTIFIC AND TECHNICAL INFORMATION DIVISION

NATIONAL AERONAUTICS AND SPACE ADMINISTRATION

Washington, D.C. 20546